Pleural Disease

17

Beatrice Feragalli, Roberta Polverosi, Anna Rita Larici, Silvia Santoro, Annemilia del Ciello, Lucio Calandriello, and Lorenzo Bonomo

Contents

Abbreviations

BPF	Bronchopleural fistula
CT	Computed tomography
MPM	Malignant pleural mesothelioma
MRI	Magnetic resonance imaging

17.1 Benign Pleural Disease

The most frequent benign pleural disease is pleural effusion; other benign conditions involving the pleura include empyema, pneumothorax, pleural plaques, and fibrothorax.

17.1.1 Pleural Effusion

A pleural effusion is an abnormal collection of fluid in the pleural space resulting from excess fluid production or decreased absorption. It is the most common manifestation of pleural disease, with etiologies ranging from cardiopulmonary disorders to symptomatic inflammatory or malignant diseases requiring urgent evaluation and treatment. The normal pleural space contains approximately 1 ml of fluid, representing the balance between hydrostatic and oncotic forces in the visceral and parietal pleural vessels and extensive lymphatic drainage. Pleural effusions result from disruption of this balance.

The parietal pleura is supplied by systemic capillary vessels and drains into the right atrium via the azygos, hemiazygos, and internal mammary

B. Feragalli (✉)
Department of Medical,
Oral and Biotechnological Sciences,
University of Chieti,
Chieti, Italy
email: b.feragalli@unich.t
R. Polverosi
Department of Diagnostic Medical Sciences
and Special Therapies, University of Padua,
Padua, Italy

A.R. Larici • S. Santoro • A. del Ciello •
L. Calandriello • L. Bonomo
Department of Bioimaging and Radiological Sciences,
Catholic University,
Rome, Italy

G. Guglielmi et al. (eds.), *Geriatric Imaging*,
DOI 10.1007/978-3-642-35579-0_17,

veins. The visceral pleura is supplied by pulmonary arterial capillaries and drains mainly into the pulmonary veins (Staub et al. 1985; Pistolesi et al. 1989). Normal pleural fluid represents interstitial fluid from the parietal pleura, which, being supplied and drained by systemic vessels, has higher capillary hydrostatic pressure than the pleural space (Sahn 1988a). Because the visceral pleura is supplied and drained by the low-pressure pulmonary circulation under normal circumstances, it probably contributes very little to pleural fluid formation, and it may absorb fluid formed by the parietal pleura (Pistolesi et al. 1989; Sahn 1988a). Lymphatic vessels play a major role in the clearance of pleural fluid (Pistolesi et al. 1989). Drainage takes place mainly through the parietal pleural lymphatics, because there is no direct communication between the lymphatic vessels of the visceral pleura and the pleural space. Increased pleural fluid may result from one of these mechanisms (Sahn 1988a): (a) increase in capillary hydrostatic pressure in the systemic and/or pulmonary circulation (congestive heart failure, superior vena cava syndrome); (b) reduction in intravascular oncotic pressure (hypoalbuminemia, cirrhosis); (c) decrease in pressure in the pleural space, preventing full lung expansion (extensive atelectasis); (d) increased permeability of the microvascular circulation or vascular disruption (inflammatory, traumatic, and neoplastic diseases of the pleura); (e) impaired lymphatic drainage from the pleural space resulting from blockage in the lymphatic system due to tumor or fibrosis; (f) increased peritoneal fluid, with migration across the diaphragm via the lymphatics or structural defect (cirrhosis, peritoneal dialysis); or (g) movement of fluid from pulmonary edema across the visceral pleura.

Pleural effusions can be divided into exudates and transudates; transudative effusions are usually caused by altered systemic factors such as increased systemic or pulmonary capillary pressures and decreased colloid osmotic pressure that result in increased filtration of fluid. This occurs in congestive left ventricular heart failure and decreased serum oncotic pressure like in liver cirrhosis. Most transudative pleural effusions have protein levels of 1.5–2.5 g/dl.

Exudative effusions occur when the pleural surface is damaged, leading to a capillary leak with increased permeability to protein; these effusions are produced by a variety of inflammatory conditions and often require more extensive evaluation and treatment than transudates. Exudates arise from pleural or lung inflammation, impaired lymphatic drainage of the pleural space, transdiaphragmatic movement of inflammatory fluid from the peritoneal space, altered permeability of pleural membranes, and increased capillary wall permeability or vascular disruption. Pleural membranes are involved in the pathogenesis of the fluid formation. In these cases, the protein level is higher than 3 g/dl, the ratio of pleural protein to serum protein is greater than 0.5, and the pleural lactate dehydrogenase to serum lactate dehydrogenase ratio is greater than 0.6 (Light 1990).

17.1.1.1 Radiological and Sonographic Features

Free pleural fluid flows to the most dependent pleural space. In upright patients, this is the subpulmonic region (Moskowitz et al. 1973), which causes an apparent elevation of the hemidiaphragm with flattening of its medial aspect (Fig. 17.1).

Approximately 75 ml of fluid is required to blunt the posterior costophrenic angle on a lateral chest radiograph. Almost 200 ml of fluid is required to blunt the lateral costophrenic angles on frontal radiographs (Moskowitz et al. 1973). On supine radiographs, it is possible to overlook large amounts of fluid, because the pleural fluid layers posteriorly. A pleural effusion must be suspected when there is increased hazy opacity on the side of the affected hemithorax without obscuration of the vascular markings (Fig. 17.2), when there is blunting of the costophrenic angles or when there is an apical cap. Loculated effusions, defined as effusions that do not shift freely in the pleural space, occur when there are adhesions between the visceral and parietal pleura (Light 1990) and are more frequently seen in exudative effusions, empyema, and hemothorax. When a loculated effusion collects within the interlobar fissures or along the mediastinum, it may simulate a mass (Fig. 17.3). Sonography is a useful tool in determining whether pleural fluid is

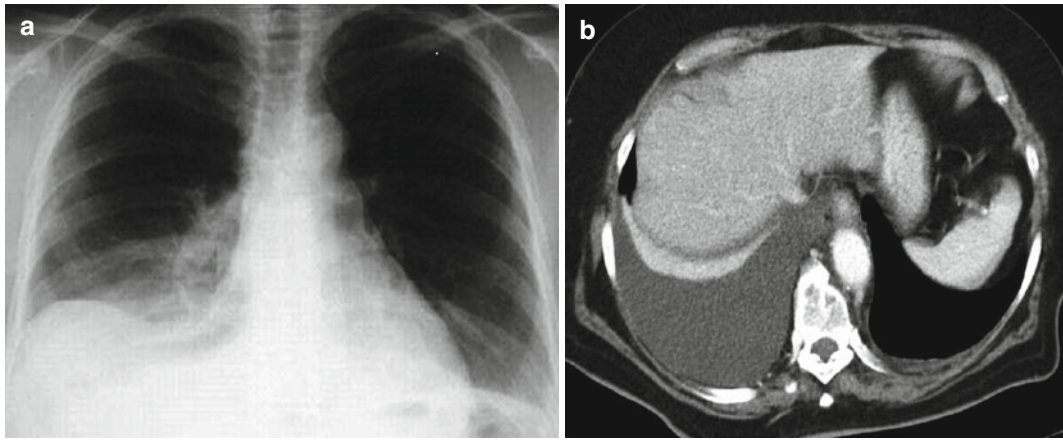

Fig. 17.1 Subpulmonary pleural effusion. Chest radiograph on frontal view (**a**) shows elevation of the right hemidiaphragm with flattening of its medial aspect. CT scan (**b**) confirms the presence of pleural effusion in the subpulmonic region

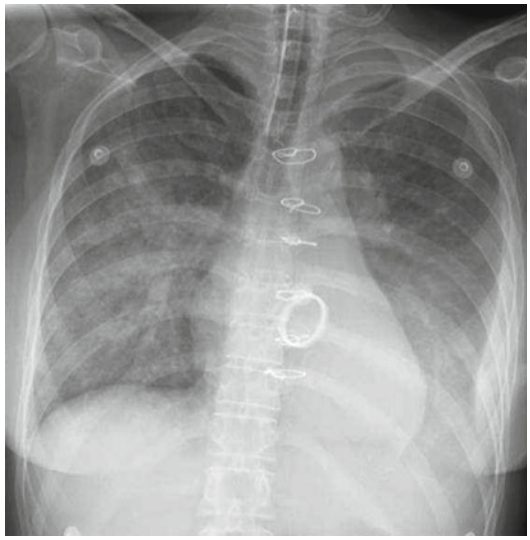

Fig. 17.2 Bilateral pleural effusion. On supine chest radiograph, there is an increased opacity of both lungs without obscuration of the vascular markings, a finding suggestive of bilateral pleural effusion; blunting of the left costophrenic angles is also present

present and also in guiding aspiration. The majority of pleural collections are identified at sonography as anechoic or hypoechoic collections delineated by the echogenic line of the visceral pleura and lung. Pleural septated effusions and those with echogenic patterns are always exudates, while hypoechoic effusions may be transudates or exudates (O'Moore et al. 1987; Yang et al. 1992). Pleural fluid can be identified on CT scans; however, CT is of limited value in differentiating transudates from exudates. Acute hemorrhage can be identified on the basis of the increased attenuation of the pleural fluid or by the presence of a fluid–fluid level (McLoud and Flower 1991a) (Fig. 17.4).

17.1.2 Empyema

Empyema is inflammatory fluid and debris in the pleural space. It results from an untreated pleural space infection that progresses from free-flowing pleural fluid to a complex collection in the pleural space. The diagnosis is made when the pleural fluid is grossly purulent, when organisms are identified on the basis of Gram stain or culture, or when the fluid has a white blood cell count greater than 5×10^9 cells/l (Light 1990). Radiographic findings are almost always the same as for any pleural collection, but certain CT findings are suggestive of empyema. The typical empyema is lenticular. Nonenhanced CT scans can demonstrate atypical pleural effusions along the mediastinum, thickened pleurae, loculations in the fissures, septa, or gas bubbles in the pleural space. Gas bubbles in the pleural space strongly suggest an empyema in the proper clinical context (i.e., in the absence of recent thoracentesis). Lung windows can demonstrate

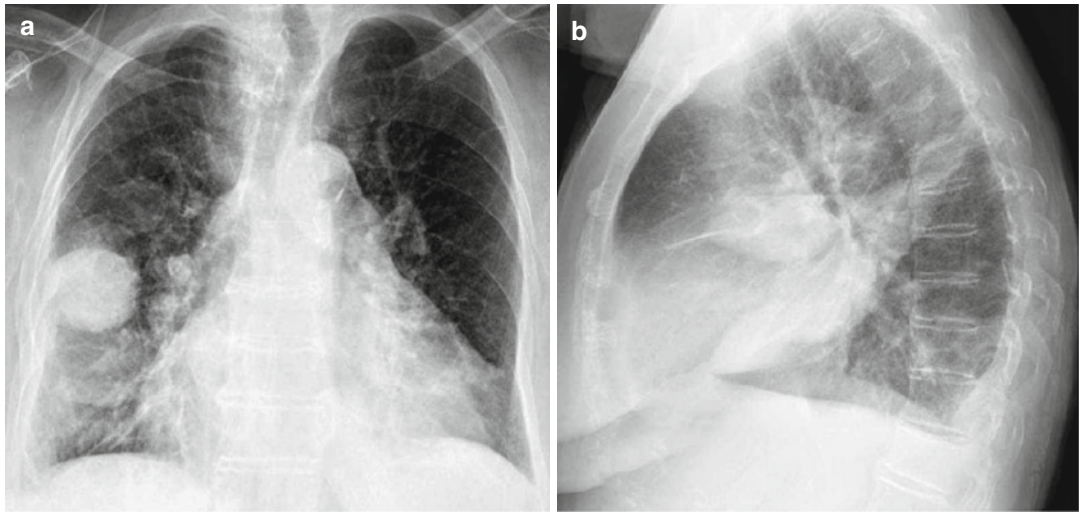

Fig. 17.3 Loculated intrafissural effusion. Chest radiograph on frontal view (**a**) shows a round well-defined opacity in the right hemithorax at the level of the small fissure simulating a mass. On the lateral view, (**b**) the opacity has a lenticular shape following interlobar fissures; these findings suggest the diagnosis of loculated intrafissural effusion

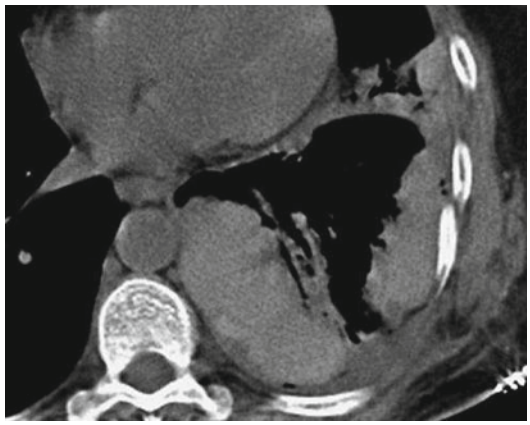

Fig. 17.4 Left acute hemothorax. Unenhanced CT scan through the lower chest depicts a left pleural effusion with increased attenuation representing an acute hemothorax

pneumonia adjacent to the abnormal pleural collection. With most empyemas, CT scans after intravenous injection of contrast medium demonstrate enhancement of the parietal and visceral pleura, the so-called split pleura (Fig. 17.5), thickening of the extrapleural subcostal tissues and increased attenuation of the extrapleural fat (Williford and Godwin 1983). It is necessary to perform a differential diagnosis with an abscess when the collection is peripheral:

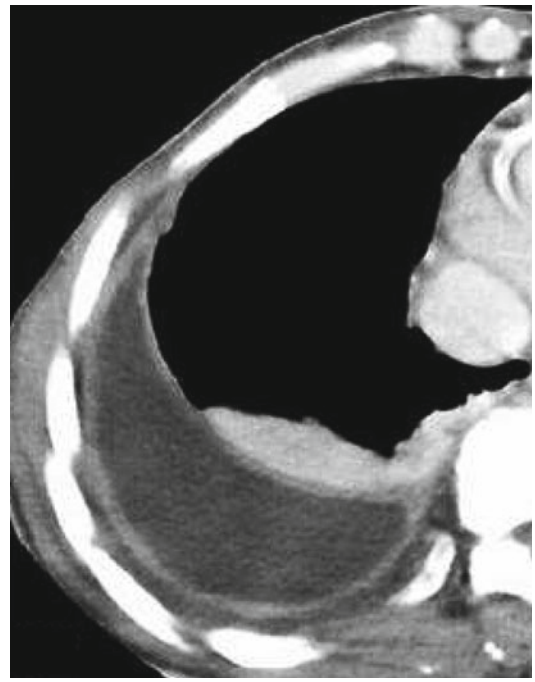

Fig. 17.5 Right pleural empyema. Enhanced CT scan shows a right loculated pleural effusion and a smooth and regular thickening both of the visceral and parietal pleura with enhancement (the so-called "spit pleura sign"); note also the expansion and increased attenuation of the extrapleural fat

an empyema generally has a lenticular shape with obtuse margins toward the chest wall, whereas a peripheral lung abscess usually has a spherical shape and forms acute angles with the chest wall. An empyema has thin, smooth walls along its inner margin; lung abscess usually has thick, irregular walls, especially internally. Finally, the adjacent lung is frequently compressed by an empyema, resulting in displacement of peripheral pulmonary vessels and bronchi, while the parenchyma surrounding a lung abscess is often infected, and the pulmonary vessels and bronchi extend directly toward the periphery of the lesion. Empyemas and associated parapneumonic effusions with pH below 7.0 or pleural fluid glucose level less than 40 mg/dl must be treated with a chest tube, inserted surgically or by image guidance with sonography or CT (McLoud and Flower 1991a). The success rates of imaging-guided drainage ranges from 70 to 90 % and are higher than those for surgical tubes guided only by the findings on the chest radiograph (Silverman et al. 1988).

17.1.3 Pneumothorax

Pneumothorax is defined as the presence of air or gas in the pleural cavity. Spontaneous pneumothorax is very rare in the elderly population but more frequent in young men; it generally occurs in people without underlying lung disease and in the absence of an inciting event. However, many patients, whose condition is labeled as primary spontaneous pneumothorax, have subclinical lung disease, such as pleural blebs, that can be detected by CT scanning. Pneumothorax secondary to pulmonary pathology is most common in elderly patients with chronic obstructive pulmonary disease, asthma, or chronic infiltrative lung disease (including idiopathic pulmonary fibrosis, sarcoidosis, eosinophilic granuloma, lymphangioleiomyomatosis). Other causes are radiation pneumonitis, silicosis, and tuberous sclerosis.

17.1.3.1 Radiological Features

Free intrapleural air moves preferentially to the less dependent pleural spaces. In the upright patient, free intrapleural air accumulates in an apicolateral location; 50 ml of pleural gas can be visible. The radiographic diagnosis of pneumothorax is based on visualization of the visceral pleura line between the radiolucent lung and radiolucent free air in the pleural space. On supine radiographs, approximately 500 ml of pleural gas is needed to visualize a pneumothorax (Tocino et al. 1985). Anteromedial and subpulmonary pneumothoraces appear to represent the majority of the air collections. In the supine position, air accumulates in front of the lung and surrounds the anterior mediastinal structures: sharp visualization of the superior vena cava (on the right) and of the left subclavian artery (on the left) are initial signs of an anteromedial pneumothorax. Infrahilar anteromedial pneumothorax accounts for a sharp delineation of the heart border and the inferior vena cava and for a deep lucent cardiophrenic sulcus (Ziter and Wescott 1981). In subpulmonary pneumothorax, a hyperlucent upper quadrant of the abdomen with visualization of the superior surface of the diaphragm can be expected; other signs are deep costophrenic sulcus and a sharp hemidiaphragm (Ziter and Wescott 1981) (Fig. 17.6). Occasionally a double-diaphragm sign is present when both the

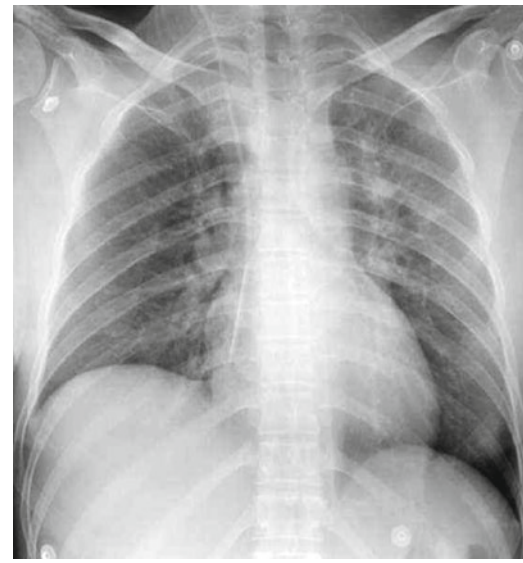

Fig. 17.6 Pneumothorax in the supine position. On frontal chest view, a deep left costophrenic sulcus and a sharp delineation of the hemidiaphragm are clearly seen suggesting the diagnosis of a left pneumothorax

anterior and the posterior surfaces of the diaphragm are surrounded by air. In patients with lung affections in whom the heart or diaphragmatic borders are not visible due to the lack of ventilation of the adjacent parenchyma, one sign of pneumothorax can be the disappearance of the "silhouette sign," which allows us to visualize the border of the heart or diaphragm once again. The disappearance of the silhouette sign is due to the interposition of the air situated in the pleural space between the affected lung and the mediastinum or the diaphragm. Apicolateral pneumothorax is uncommon in a supine radiograph and suggests that a large volume of pleural air has accumulated and has displaced the visceral pleura medially. Because of the difference in compliance of the lung when affected by parenchymal diseases like pneumonia or adult respiratory distress syndrome, segments of the lung may collapse under pneumothorax, whereas others more severely involved are seen beyond the pneumothorax; therefore, the presence of lung markings beyond a pleural line does not exclude pneumothorax in a supine plain film. When the amount of air accumulated is small, the first sign of apicolateral pneumothorax in the right side is a lack of contact between the minor fissure and the chest wall (Ziter and Wescott 1981). It is important to bear in mind that skinfolds, dressings, tubing, and bags can mimic pneumothorax on some images. Care must be taken when obtaining chest radiographs to minimize these artifacts.

A tension pneumothorax is a life-threatening condition that develops when air is trapped in the pleural cavity under positive pressure (Gilbert and McGrath 1993), displacing mediastinal structures and compromising cardiopulmonary function. Prompt recognition of this condition is life saving. Because tension pneumothorax occurs infrequently and has a potentially devastating outcome, a high index of suspicion and knowledge of basic emergency thoracic decompression procedures are important for all healthcare personnel. Immediate decompression of the thorax is mandatory when tension pneumothorax is suspected. Signs of tension pneumothorax are diaphragm inversion, displacement of the anterior junction line to the contralateral side, or displacement of the azygoesophageal recess. The sign that correlates best with clinical findings of tension pneumothorax is flattening of the heart border and other vascular structures. This sign is due to the impairment to the normal venous return to the heart that occurs in tension pneumothorax (Gilbert and McGrath 1993).

17.1.4 Pleural Plaques

Pleural plaques constitute the most frequent benign pleural pathology in asbestos-exposed patients and are radiologically detectable in 20–60 % of workers exposed to high concentrations of asbestos. A history of asbestos exposure may be demonstrated in over 80 % of subjects with bilateral pleural plaques. Pleural plaques represent circumscribed collections of hyalinized collagen in the submesothelial layer of the parietal pleura of chest wall or diaphragm; they rarely affect mediastinal pleura. Pleural plaques almost always involve the parietal pleura alone, but occasionally they may be seen in the visceral pleura and in the interlobular fissures. They generally appear 15–20 years after the initial exposure. The pathogenesis of asbestos-related pleural plaques is unknown; it is presumed that asbestos fibers penetrate the visceral pleura and irritate the parietal pleura, inciting collagen deposition. The thickness of plaques can vary from 1 mm to more than 10 mm. Plaques are thicker over the ribs than over the intercostal spaces.

17.1.4.1 Radiological Features

On chest radiographs, these lesions appear as focal areas of pleural thickening, usually less than 1 cm thick, and predominantly localized posterolaterally along the inferior costal margins and at the diaphragmatic level. They are usually bilateral and tend to be asymmetrically distributed; when monolateral (25 % of cases), for reasons as yet unknown, they are prevalently left-sided. Pleural plaques have a tendency to calcify. Forty years after the initial exposure to asbestos, almost 40 % of these people exhibit radiologically obvious pleural calcifications. They may appear punctate, linear, or occasionally

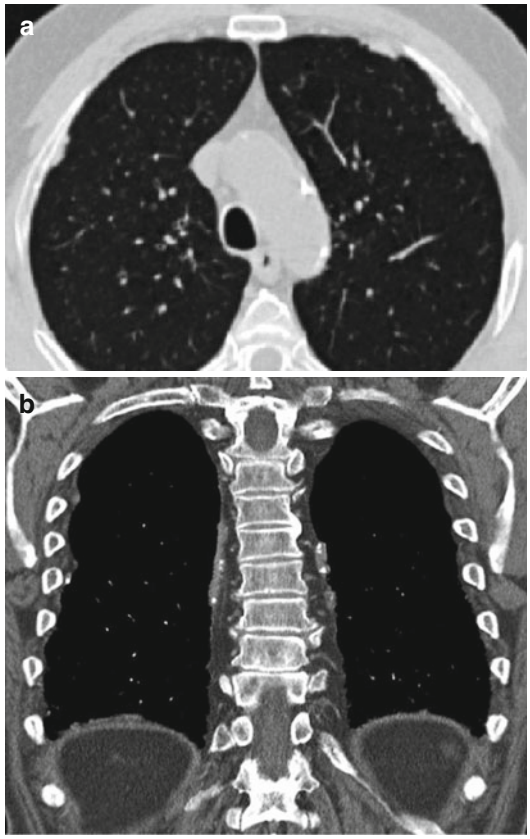

Fig. 17.7 Pleural plaques in a patient with history of asbestos exposure. Axial CT scan (**a**) shows focal areas of pleural thickening with bilateral and asymmetric distribution along the costal pleural surfaces. On coronal reformatted image, (**b**) the plaques appear partially calcified and are also seen along the diaphragmatic pleura

"cakelike," especially when located along the diaphragm surfaces. Less commonly calcified plaques may be pedunculated, in which case they may be mistaken for intraparenchymal nodules (Muller 1993). CT facilitates the successful detection and location of pleural plaques because the cross-sectional images are free from overlapping (Fig. 17.7). It can also define subpleural fat deposits that mimic plaques on plain radiographs. Radiological findings that are suggestive of extrapleural fat rather than pleural plaques include a bilateral location among the midlateral chest wall and a symmetric distribution. Some authors have shown that the combination of bilateral abnormalities and posterolateral plaques at least 5 mm thick or bilateral calcified diaphragmatic plaques has a 100 % positive predictive value for the diagnosis of asbestos-related disease. Although pleural plaques per se are asymptomatic and not premalignant, detection of pleural plaques is important for three main reasons: (a) in patients with associated interstitial disease, the presence of these lesions, in the appropriate clinical setting, strongly suggests the diagnosis of asbestosis; (b) they are virtually pathognomonic of asbestos exposure and thus are important diagnostic clues suggesting an increased risk of developing malignant pleural mesothelioma; and (c) they may serve as encouragement to stop smoking because of the synergistic interaction between asbestos exposure and smoking in the development of lung cancer (Muller 1993).

17.1.5 Fibrothorax

Fibrothorax, almost always due to previous empyema, is easily detected as a thick, calcified pleural rind on both plain radiographs. Calcified fibrothorax in older patients is particularly likely to be tuberculous in origin. The list of possibilities can be narrowed down given a history of therapy for tuberculosis, although such a history is frequently lacking (Hulnick et al. 1983). Rarely, tuberculous pleurisy progresses to become chronic tuberculous empyema, which may be defined as persistent, grossly purulent pleural fluid containing numerous tubercle bacilli. Since the advent of chemotherapy, this is usually seen secondary to incomplete medical treatment, which sometimes leads to the development of resistant organisms (Gallardo et al. 2000). Tuberculous empyema is often asymptomatic and sometimes does not become apparent until many years after the episode of acute pleurisy. During this period, tubercle bacilli remain dormant within the calcified pleural space and are later reactivated. CT, which differentiates fluids from soft tissues and calcifications, can identify collections of pleural fluid within a calcified fibrothorax. These findings are the most accurate indicator of active infection. In addition, CT can be of value in diagnosing complications that may arise from chronic tuberculous empyema,

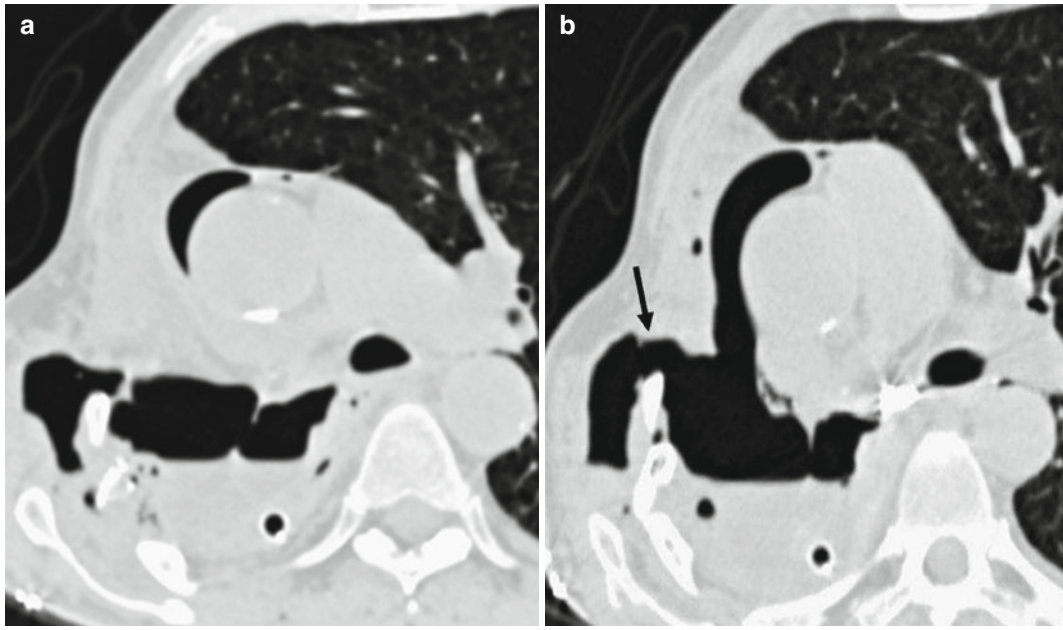

Fig. 17.8 Empyema necessitatis. Axial CT images (**a**, **b**) demonstrate a multiloculated collection in the right pleural cavity with a communication between the empyema and the chest wall and a subcutaneous air-fluid level (*arrow* in **b**)

specifically bronchopleural fistula (BPF) and empyema necessitatis (EN). Although BPF is decreasing in frequency, it is still a serious complication of pulmonary resection and inflammatory diseases of the lungs. Tuberculous residual derangement in pulmonary or pleural architecture, spontaneous or iatrogenic, predisposes to the development of BPF. Fibrothorax appears to be the most common source of late BPF formation, while, during the active disease, rupture of a pulmonary cavity in the pleural space is more common. BPF may present clinically in various forms, ranging from incidental radiographic discovery to life-threatening acute pneumothorax. Radiographically, BPF usually presents as a new pleural air-fluid level, and sometimes with a tension pneumothorax. Diagnosis is often made by the correlation of sequential changes in chest radiographs. The presence or absence of an active infection is crucial in selecting appropriate medical treatment. The introduction of a drainage tube alone can lead to closure of the fistula. If the fistula does not close with tube drainage in a few weeks, a definitive operation is recommended (Hulnick et al. 1983). EN is an uncommon complication of an empyema in which the inflammatory mass spontaneously bores its way from the pleural cavity into the soft tissues of the thoracic wall, forming a subcutaneous abscess, which may or may not open to the skin. The most common etiology is tuberculosis. The most common clinical presentation is a mass in the thoracic wall that is sometimes accompanied by a cutaneous fistula. The chest radiograph usually shows signs of chronic pleural disease with pleural thickening, which may be calcified. A subcutaneous mass associated with pleural empyema should be considered suspicious for EN. CT is very useful and is diagnostic when it shows a pleural collection with thickened often calcified pleural wall, associated with a mass in the thoracic wall (Fig. 17.8).

17.2 Malignant Pleural Disease

Malignant pleural disease is a common clinical problem, as about 25 % of all pleural effusions in elderly patients have a neoplastic origin Feragalli B et al. 2003).

The pleura may be involved by one of several primary or secondary malignant tumors. Primary tumors account for about 10 % of pleural malignancies and are malignant pleural mesothelioma, localized fibrous tumor, and pleural sarcoma. Secondary tumors account for about 90 % of pleural neoplasms; the principal causes are adenocarcinoma or, less frequently, lymphoma and thymoma.

Depending on the location, size, and underlying histologic features, pleural tumors may produce a spectrum of findings; CT is the best method for characterizing location and composition of pleural masses and is particularly useful in distinguishing pleural from peripheral pulmonary lesions.

17.2.1 Primary Tumors

17.2.1.1 Malignant Pleural Mesothelioma

Malignant pleural mesothelioma (MPM) is the most common primary neoplasm of the pleura that typically affects individuals occupationally exposed to asbestos through a variety of industries.

Epidemiology and Etiology

MPM is an important health problem both because its incidence has increased over the past 30 years and because of the diagnostic, clinical, and therapeutic challenges it poses (Damhuis and Planteydt 1995; Peto et al. 1995; Aberle and Barnes 1991). Approximately 2,000–3,000 cases of MPM occur in the United States each year (Aberle and Barnes 1991), and the incidence is expected to rise till approximately 2020 (Peto et al. 1995). Men are more frequently affected, and the male to female ratio is 2–6:1. The peak of incidence occurs between the sixth and seventh decade of life (Pisani et al. 1988); MPM is extremely rare in childhood (Fraire et al. 1988; Kane et al. 1990).

The association between MPM and asbestos fibers was established in 1960 by Wagner et al. (1960) in a landmark study which identified a clear relationship between occupational exposure to crocidolite and the development of mesothelioma. Thereafter, this association was confirmed by numerous studies (Antman 1980; Churg 1988; Craighead et al. 1982; Mossman and Churg 1998; Roggli et al. 1992) that demonstrated a high incidence of MPM among patients with prolonged asbestos exposure and a beginning was made to abandon the production and processing of asbestos material. Approximately 80 % of MPM cases occur in individuals occupationally exposed to asbestos (McDonald and McDonald 1980; Hammar 1994a, b); the lifetime risk of developing mesothelioma for asbestos workers has been estimated at about 10 % (Selikoff et al. 1980). The incidence of MPM is higher in subjects with continuous exposure compared to occasional exposure; nonetheless, even brief (under 1 year) or indirect exposures (such as contact with the clothing of an exposed worker) may produce the tumor. The highest incidences are found in shipyard and construction workers, in asbestos miners and manufacturers, and in heating trade and insulation workers (McDonald and McDonald 1980; Huncharek 1992).

The latency period for development of MPM is about 35–40 years after initial exposure; the incidence peak occurs later than asbestos-related lung cancer (25–30 years) and earlier than asbestosis (40–45 years). Unlike asbestosis and lung cancer, the incidence of MPM does not decrease after reaching its peak but remains steady.

Asbestos minerals can be divided in the serpentines (chrysotile, the so-called "white asbestos," and anthophyllite) and the amphiboles (crocidolite, the so-called "blue asbestos"; amosite, the so-called "brown asbestos"; and tremolite). The carcinogenicity appears to be related to the length-to-diameter ratio of asbestos fibers; fibers with the highest ratio being the most carcinogenic. In general, the amphiboles have the highest ratio, and epidemiologic data confirms their malignant potential (Mossman and Churg 1998; Rudd 1996). The amphiboles appear to be 15 times more potent than chrysotile in the development of mesothelioma (Miller et al. 1996). The microscopic marker of heavy prior asbestos exposure is the presence in the sputum of so-called "asbestos bodies," a type of ferruginous bodies resulting from the deposition of iron–protein

complexes on asbestos fiber cores. Macroscopic markers of asbestos exposure are pleural plaques (Greenberg 1992; Hillerdal 1994). As we described before, pleural plaques radiologically appear as focal areas of pleural thickening, typically less than 1 cm thick, that affect the parietal pleura; the visceral pleura is rarely affected. The plaques first appear 15–20 years after the initial asbestos exposure. There is no evidence that these lesions are premalignant or precursors of MPM; the presence of plaques, however, does suggest an increased probability of MPM occurring (Hillerdal 1994).

About 20 % of patients with mesothelioma have no history of asbestos exposure nor evidence of asbestos fibers in their lungs, and, consequently, other etiologic factors have been implicated including exposure to other mineral fibers (zeolite), chronic inflammation, genetic factors, radiation exposure, viruses (Simian virus 40), and exposure to other nonfibrous minerals and organic chemicals (polyurethane, ethylene oxide, polysilicone) (Hammar et al. 1989; Carbone et al. 1997; Peterson et al. 1984; Sahin et al. 1993; Hillerdal and Berg 1985; Baas et al. 1998).

Clinical Features

Most patients present relatively late with symptoms since the onset is usually insidious. The most frequently reported complaints are localized chest pain (70 %), as a result of growth in the chest wall, and dyspnea (68 %) due to the presence of a pleural effusion. Weight loss, coughing, and fever are also present in a large proportion of patients. Secondary hypertrophic osteoarthropathy occurs in less than 10 % of patients (Antman 1980). Laboratory analysis may reveal thrombocytosis (more than 400,000 platelets/mm^3) which occurs in 34–41 % of patients (Ruffie 1992). Intermittent hypoglycemia is found in less than 10 % of patients.

Pathological Features

MPM manifests most commonly as multiple tumor masses that involve the parietal and visceral pleural surfaces with greater involvement of the parietal than visceral layer. The tumor may progress to thick sheet like or confluent masses, with resultant lung encasement. Greater involvement of the inferior hemithorax is probably due to gravitational factors. A pleural effusion, whether exudative, bloodstained, or frankly hemorrhagic, is present in about 60 % of patients at diagnosis. Chest wall and mediastinal involvement, including pericardial and cardiac invasion, may occur in advanced disease. Tumor growth along needle tracks and scars that penetrate the chest wall have been documented. The diaphragm is frequently infiltrated; tumor extension into the peritoneal cavity is identified in at least one-third of autopsies. Lymphatic and hematogenous metastases occur more frequently than previously supposed (Huncharek 1994; Huncharek and Smith 1988) and are found at autopsy in more than half of MPM cases (Huncharek 1994).

Microscopically, MPM is generally divided into three histologic categories: epithelioid, sarcomatoid, and biphasic. Epithelioid mesothelioma constitutes approximately 55–65 % of malignant mesotheliomas; it may be difficult to distinguish from peripheral adenocarcinoma of the lung with pleural invasion or adenocarcinoma metastatic to the pleura. Techniques other than hematoxylin–eosin staining are needed to make the correct diagnosis, including histochemical staining, immunohistochemical staining, and electron microscopy (Miller et al. 1996; Wick et al. 1990). The sarcomatoid variant constitutes approximately 10–15 % of MPM and must be differentiated from a true sarcoma such as osteosarcoma or chondrosarcoma. The remaining mesotheliomas (20–35 %) fall into the biphasic category, which evinces features of both epithelioid and sarcomatoid mesotheliomas.

Radiographic Features

The most indicative plain radiographic findings of MPM are irregular, nodular opacities around the periphery of the lung, associated with ipsilateral pleural effusion (30–95 %) (Wechsler et al. 1983). However, it should be remarked that pleural thickening, especially when focal and circumscribed, cannot be identified on chest radiograph and, consequently, a monolateral pleural effusion can often be the only radiographic sign of an MPM. Unlike pleural effusion unrelated to pleural

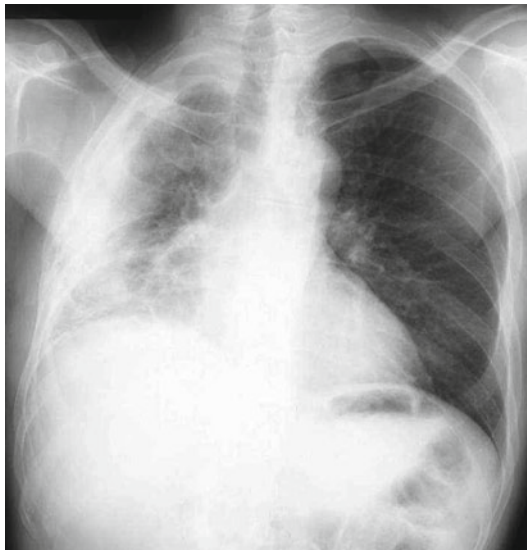

Fig. 17.9 Right MPM in a 55-year-old woman with no history of asbestos exposure. PA chest radiograph shows right pleural effusion and irregular pleural thickening with extension to the major fissure, encasing the lung and contracting the right hemithorax

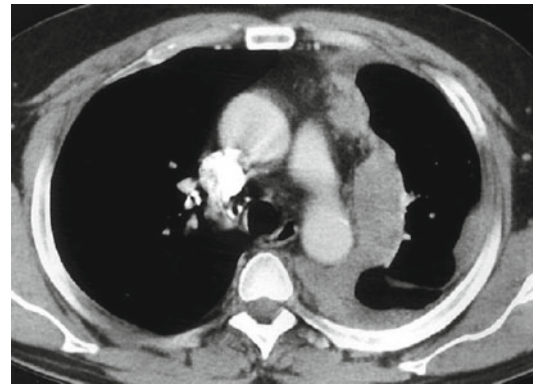

Fig. 17.10 Left MPM in a 59-year-old man with history of asbestos exposure. Enhanced CT scan through the upper chest shows circumferential, irregular, and left-sided pleural thickening with involvement of the fissure. Mediastinal pleura appears particularly thickened at this level where the neoplastic tissue infiltrates the mediastinal fat without any sign of blood vessel involvement

malignancies, pleural effusion in MPM is characteristically not associated with contralateral shift of the mediastinum because of the restrictive action of the pleural tumor peel. Instead there may be evidence of volume loss on the affected side, with narrowing of the intercostal spaces, elevation of the hemidiaphragm, and ipsilateral shift of the mediastinum (Fig. 17.9). Alternatively the mediastinum may be fixed in the midline. Distinct pleural masses without effusion are identified in less than 15 % of patients on their initial chest radiograph. It should be recalled, however, that radiography does not always allow easy and precise definition of the pleural or parenchymal localization, just as pleural thickening may be erroneously diagnosed even in the absence of this disease. False positives may be due to thickening of the subpleural fat or to prominence of intercostal muscles; symmetric radiographic findings may sometimes suggest the correct diagnosis and exclude pleural disease. In conclusion, plain chest radiography has low specificity and sensitivity in diagnosing pleural diseases, particularly MPM; recidivant monolateral pleural effusion, especially if associated with ipsilateral volume loss, should raise the suspicion of MPM, thus indicating that CT is needed.

CT Features

CT has been shown to be superior to chest radiography in identifying and characterizing pleural disease. The tumor often shows a widespread nodular thickening surrounding the lung, spreading into the fissures and extending into the mediastinum (Fig. 17.10). In a study of 50 patients, Kawashima and Libshitz (1990) reported the most frequent CT findings of MPM: diffuse or nodular pleural thickening (92 % of patients), thickening of the interlobular fissures (86 %), pleural effusion (74 %), loss of volume of the involved hemithorax (42 %), pleural calcifications (20 %), and chest wall invasion (18 %). In a more recent study, other authors (Seely et al. 2009) reviewed CT findings of 92 patients with biopsy-proved MPM. They found that all the patients had pleural thickening that was nodular in 79 patients (86 %) and mediastinal in 87 (95 %); ipsilateral volume loss was seen in 42 patients (46 %) and pleural effusion in 80 patients (87 %).

Detection of the above signs raises the problem of differentiating MPM from other benign or malignant pleural diseases also manifesting with pleural effusion and thickening, including fibrothorax, asbestos-related pleural fibrosis,

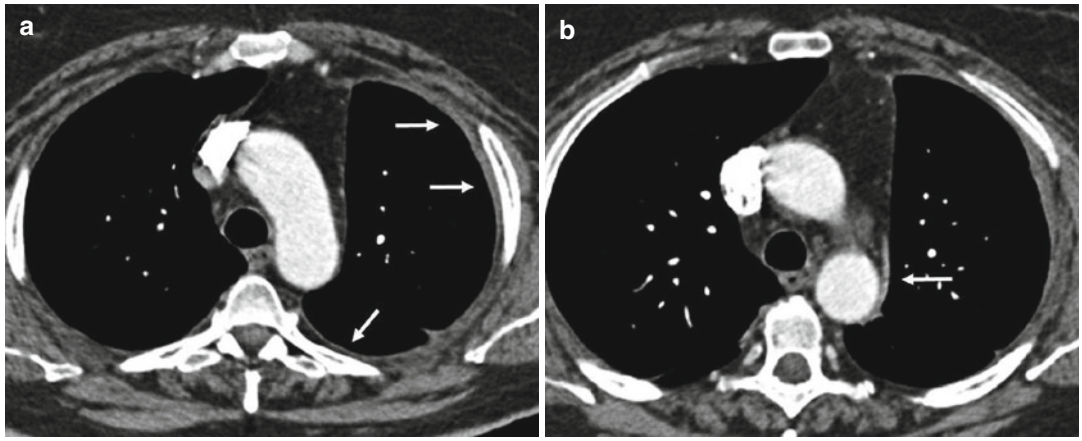

Fig. 17.11 Fifty-five-year-old woman with early MPM. CT scans show a minimal thickening of the left parietal pleura (*arrows* in **a**) associated with a minimal and focal thickening of the ipsilateral mediastinal pleura (*arrow* in **b**) and a mild volume loss of the hemithorax. Even when it is smooth and regular, as in this case, the involvement of mediastinal pleura is suspect for MPM

empyema, infections (tuberculosis, fungal, actinomycosis), and pleural metastasis. Leung et al. (1990) have shown that, despite this overlap, CT can play a major role in distinguishing malignant from benign pleural disease in consideration of the following high specific signs: (*a*) circumferential pleural thickening (specificity 100 %, sensitivity 41 %), (*b*) nodular pleural thickening (specificity 94 %, sensitivity 51 %), (*c*) parietal pleura thickening of more than 1 cm (specificity 94 %, sensitivity 36 %), and (*d*) mediastinal pleural involvement (specificity 88 %, sensitivity 56 %). Twenty-eight of 39 malignant cases (sensitivity 72 % and specificity 83 %) were identified correctly on the basis of the presence of one or more of these criteria. These features may be seen in mesothelioma and in metastatic pleural disease but are unusual in benign pleural disease. There is a close correlation between these signs and pathology. Whereas MPM tends to involve the entire pleural surface, reactive pleurisy usually does not affect the mediastinal pleura (except in case of tuberculous empyema which, when extensive, may involve the mediastinal pleura); for this reason, it is important to remember that mediastinal pleural thickening and circumferential pleural thickening, also when minimal and focal, should raise suspicion of MPM especially when associated with pleural effusion and/or ipsilateral volume loss (Figs. 17.11 and 17.12).

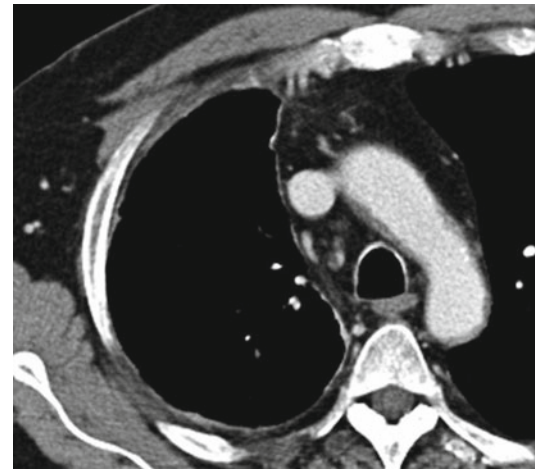

Fig. 17.12 Sixty-seven-year-old man with early MPM. Axial enhanced CT scan displays minimal pleural thickening with circumferential appearance, suggestive of MPM

More recently, other authors (Hierholzer et al. 2000) described signs indicative of malignant pleural disease, finding similar results to those reported above, except for pleural thickening more than 1 cm that was seen in both malignant and benign pleural disease with no statistically significant differences.

The presence of pleural calcifications suggests a benign process. In the series by Lung, calcifications were seen in 16 of 35 patients with benign pleural thickening and in only 3 of 39

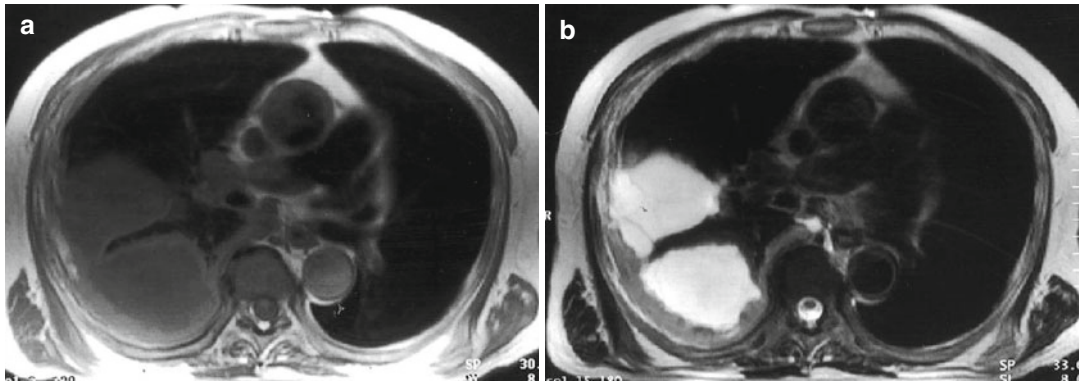

Fig. 17.13 MPM of the right lung in a 68-year-old man. Axial T1-weighted MRI (**a**) demonstrates irregular pleural thickening of moderate signal intensity and loculated pleural effusions of lower signal intensity. Axial T2-weighted image at a similar level (**b**) allows differentiation between the tumor, which has increased signal intensity relative to that of the chest wall musculature, and the pleural effusion, which has very high signal intensity

patients with malignant pleural disease. Rib destruction and frank chest wall invasion are good indicators of malignancy; however, some infectious process, such as actinomycosis, tuberculosis, and nocardiosis, very rarely can invade the chest wall, but usually at a single focus rather than at multiple sites, as seen with malignant disease (Miller et al. 1996).

To conclude, CT is highly sensitive in identifying pleural disease. Most of the time, it allows differentiation between benign and malignant pleural lesions, whereas it does not always enable differentiation between MPM and pleural metastasis when these involve only one hemithorax.

MRI Findings

MPM has intermediate signal intensity on T1-weighted images, similar to that of chest wall muscles. On T2-weighted images, MPM has increased signal intensity relative to that of the adjacent chest wall musculature with focal areas of very high signal intensity due to pleural fluid (Hierholzer et al. 2000; McLoud and Flower 1991b; Montalvo et al. 1991) (Fig. 17.13). Like CT, MRI scans allow identification of pleural thickening, involvement of the interlobar fissures, and the craniocaudal extension of the tumor. The signal intensity of pleural lesions has also been analyzed by Falaschi et al. (1996) who assessed the capability of MRI to differentiate malignant from benign pleural lesions. The authors found that high signal intensity on T2-weighted images was observed in all malignant lesions, whereas only two benign lesions in their series displayed this signal. The authors concluded that high signal intensity on T2-weighted images had a good diagnostic accuracy in differentiating malignant from benign pleural lesions, showing a sensitivity of 100 % and a specificity of 87 %. The negative predictive value was 100 % which implies that the presence of low signal intensity in sequences with long repetition time (TR) is a reliable sign of benignity and is related to the fibrosis characteristic of benign disease. In their more recent study, Hierholze and colleague (Hierholzer et al. 2000) confirmed that high signal intensity in relation to intercostal muscles on T2-weighted and/or contrast-enhanced T1-weighted images is significantly suggestive for malignant disease. Using morphologic features in combination with the signal intensity features, MRI had a sensitivity of 100 % and a specificity of 93 % in the detection of pleural malignancy. It can therefore be inferred that, in identifying and characterizing pleural lesions, MRI may be used as an adjunct to CT in the presence of doubtful findings.

Diagnostic Thoracoscopy

Diagnostic thoracoscopy is indicated in any patients without a precise histopathological diagnosis in whom clinical and laboratory findings raise the suspicion of MPM. In a study of 188 patients with MPM, Boutin et al. (Boutin and

Rey 1993; Boutin et al. 1993) compared the sensitivity of the diagnostic techniques currently used in the diagnosis of MPM. They reported the following sensitivity rates: (*a*) pleural fluid cytology, 26 %; (*b*) percutaneous needle biopsy, 20.7 %; (*c*) pleural fluid cytology and needle biopsy, 38.7 %; and (*d*) thoracoscopic biopsy, 98.4 %. Medical or surgical thoracoscopy has therefore become the gold standard for the cytological–histological diagnosis of MPM, and exploratory thoracotomies, burdened by higher mortality and morbidity rates, have been almost completely abandoned.

Prognosis and Staging

MPM is a usually fatal primary neoplasm. In fact once malignant mesothelioma is diagnosed, the typical course is rapid progression to death, usually of local disease: the mean survival time after diagnosis is approximately 11 months in patients treated with conventional therapies. Some studies have demonstrated that survival was improved in patients who had extrapleural pneumonectomy followed by radiation and chemotherapy (Sugarbaker et al. 1991, 1999; Pass 1994). Extrapleural pneumonectomy is performed in patients with tumor confined to the affected hemithorax and provides for resection of ipsilateral pleura, lung, pericardium, and diaphragm. Accurate preoperative staging is required for selection of patients who could benefit from multimodality treatment and to allow comparison between different studies. Although a number of staging systems have been proposed in the past, many described only advanced malignant pleural mesothelioma (Boutin et al. 1993; Butchart et al. 1976; Sugarbaker et al. 1993) further limiting uniformity of approach. In 1994, an international TNM staging (International Mesothelioma Interest Group 1995) for MPM was proposed by the International Mesothelioma Interest Group (Table 17.1). The TNM descriptors are primarily based on surgical and pathologic findings but are also potentially applicable to staging by CT and MRI (Patz et al. 1996) so that patients can be selected accurately for either surgical resection or nonsurgical therapy. T1a describes an early tumor that involves only the ipsilateral parietal pleura with or without tumor on the diaphragmatic or mediastinal pleura. T1b describes a slightly more advanced tumor that involves all pleural surfaces, including the visceral pleura. T2 designates a tumor that cannot be fully removed without resecting the underlying lung. Usually the diaphragmatic muscle is also involved. T3 describes a locally advanced tumor that is still amenable to surgical resection of all gross disease. In addition to involvement of all the pleural surfaces, there may be areas of tumor extension into the endothoracic fascia or the mediastinal fat. There may be a nontransmural involvement of the pericardium. A solitary, completely resectable focus of tumor extending directly into the chest wall is also included in the T3 category; this focus usually occurs in patients who have a tumor implant in the chest wall at the site of a previous diagnostic thoracentesis, pleural biopsy, or thoracoscopy. T4 designates a locally advanced and technically unresectable tumor. In addition to involvement of all the pleural surfaces, T4 is characterized by features including diffuse extension of tumor into the chest wall, direct extension through the diaphragm to the underlying peritoneum, or direct extension to the contralateral pleura, the mediastinal organs, the spine, the myocardium, or the internal surface of the pericardium.

The descriptors for N and M status are identical to those used in the International Lung Cancer Staging System. In particular, with regard to N staging, it is important to emphasize that, although the classification is still equal to that for lung cancer, many differences exist in prevalence and pattern of lymph node metastasis in MPM. In the recent study of Seely et al. (2009), the authors found a high incidence of extrapleural node involvement given that the parietal pleura normally drains into these nodes: in their population of 92 patients with MPM, internal mammary lymphadenopathy was observed in 52 % of cases, cardiophrenic lymphadenopathy in 46 %, retropleural lymphadenopathy in 33 %, and mediastinal adenopathy in 23 %. It is of particular relevance that no patients had enlarged hilar nodes since they drain the lung and visceral but not parietal pleura. Similar results were found in

Table 17.1 New international staging system for diffuse MPM

T1a	Tumor limited to the ipsilateral parietal pleura, including mediastinal and diaphragmatic pleura No involvement of the visceral pleura
T1b	Tumor involving the ipsilateral parietal pleura, including mediastinal and diaphragmatic pleura Scattered foci of tumor also involving the visceral pleura
T2	Tumor involving each of the ipsilateral pleural surfaces (parietal, mediastinal, diaphragmatic, and visceral pleura) with at least one of the following features: Involvement of diaphragmatic muscle Confluent visceral pleural tumor (including the fissures) or extension of tumor from visceral pleura into the underlying pulmonary parenchyma
T3	Locally advanced but potentially resectable tumor. Tumor involving all of the ipsilateral pleural surfaces (parietal, mediastinal, diaphragmatic, and visceral pleura) with at least one of the following features: Involvement of the endothoracic fascia Extension into the mediastinal fat Solitary, completely resectable focus of tumor extending into the soft tissues of the chest wall Nontransmural involvement of the pericardium
T4	Locally advanced technically unresectable tumor. Tumor involving all of the ipsilateral pleural surfaces (parietal, mediastinal, diaphragmatic, and visceral pleura) with at least one of the following features: Diffuse extension or multifocal masses of tumor in the chest wall, with or without associated rib destruction Direct transdiaphragmatic extension of tumor to the peritoneum Direct extension of tumor to the contralateral pleura Direct extension of tumor to one or more mediastinal organs Direct extension of tumor into the spine Tumor extending through to the internal surface of the pericardium with or without a pericardial effusion or tumor involving the myocardium
NX	Regional lymph nodes cannot be assessed
N0	No regional lymph node metastases
N1	Metastases in the ipsilateral bronchopulmonary or hilar lymph nodes
N2	Metastases in the subcarinal or the ipsilateral mediastinal lymph nodes, including the ipsilateral internal mammary nodes
N3	Metastases in the contralateral mediastinal, contralateral internal mammary, and ipsilateral or contralateral supraclavicular lymph nodes
MX	Presence of distant metastases cannot be assessed
M0	No distant metastases
M1	Distant metastases present
Stage Ia	T1aN0M0
Stage Ib	T1bN0M0
Stage II	T2N0M0
Stage III	Any T3M0, N1M0, and N2M0
Stage IV	Any T4, N3, and M1

another recent study (Abdel Rahman et al. 2008) in which the authors found that the mechanism of spread of MPM to hilar nodes may be through lung invasion and not direct spread from the pleura. This observation confirms that extrapleural, cardiophrenic, and internal mammary nodes should be considered the primary stations in patients with mesothelioma (Fig. 17.14), whereas hilar node metastasis necessitates lung invasion first. Consequently, the pattern of nodal metastases

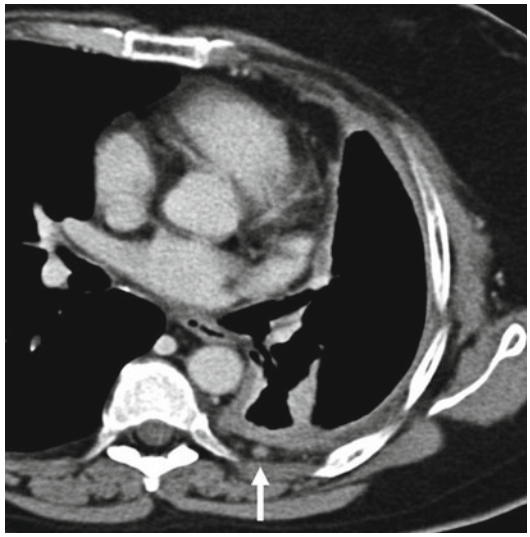

Fig. 17.14 MPM presenting with left hemithorax volume loss and diffuse pleural thickening. Notice the small nodes in the extrapleural space (*arrow*). In a patient with suspected MPM, the presence of these nodes can help in a more confident diagnosis

in MPM is different from that of lung cancer, and a revision of TNM classification should be considered because patients with positive hilar nodes should be classified to a higher stage than those with mediastinal nodal metastases.

To stage MPM by imaging, it appears that CT and MRI cannot always distinguish among T1a, T1b, and T2 because these techniques cannot usually differentiate parietal from visceral involvement or consistently detect diaphragmatic muscle invasion (Patz et al. 1996). However, both CT and MRI may have an impact in distinguishing T3 (potentially resectable MPM) from T4 (technically unresectable MPM) disease. In imaging, the tendency is to under stage the true extent of MPM; under staging may be less important in the resectable stages (T1–T3) but assumes greater importance in the diagnosis of T4 (unresectable) disease.

According to literature, the CT and MRI criteria for resectability include (*a*) lesion limited to one hemithorax; (*b*) preservation of extrapleural fat planes, muscles, and intercostal spaces; (*c*) normal CT attenuation values and MRI signal intensity characteristic of mediastinal structures adjacent to the tumor; and (*d*) a smooth and regular inferior diaphragmatic surface with a clear fat plane between the diaphragmatic surface and adjacent abdominal organs (Fig. 17.15). Imaging criteria for unresectability include (*a*) invasion of the extrapleural soft tissue or fat; (*b*) infiltration–displacement of ribs by tumor or evidence of bone destruction, (*c*) CT or MRI findings suggestive of invasion of essential mediastinal structures, tumor surrounding more than 50 % of the circumference of a vascular structure or transmural infiltration of the pericardium with obliteration of the endopericardial fat tissue (Fig. 17.16); and (*d*) tumor encasing the diaphragm with irregular appearance of the abdominal diaphragmatic surface (Fig. 17.17). In a study of 41 patients with MPM, Patz et al. (1992) compared the value of CT and MRI in predicting resectability and concluded that CT and MRI provide similar information in most cases. The sensitivity of CT and MRI in evaluating the resectability of the tumor at the level of diaphragm, chest wall, and mediastinum was, respectively, 94, 93, and 100 % for CT and 100, 100, and 92 % for MRI. The specificity of both modalities was rather poor, ranging from 25 to 50 %, probably as a result of the small number of patients studied. The authors concluded that CT and MRI have similar accuracy in predicting MPM resectability and therefore, because of its widespread availability, CT is currently regarded as the initial study for staging MPM, limiting MRI to doubtful cases.

In another series, Heelan et al. (1999), in their review of 95 patients with MPM, found that CT and MRI are of nearly equivalent diagnostic accuracy in staging MPM. MRI has been demonstrated superior to CT in revealing solitary foci of chest wall invasion and endothoracic fascia involvement and in showing diaphragmatic muscle invasion. However, this advantage does not affect surgical treatment, and moreover, various thoracic motion artifacts on MRI had been only partially avoided by cardiac gating and respiratory compensation. For these reasons, the authors concluded that CT should be considered the standard preoperative cross-sectional technique for staging malignant pleural mesothelioma. MRI should be reserved for problem solving in specific cases, such as for a patient

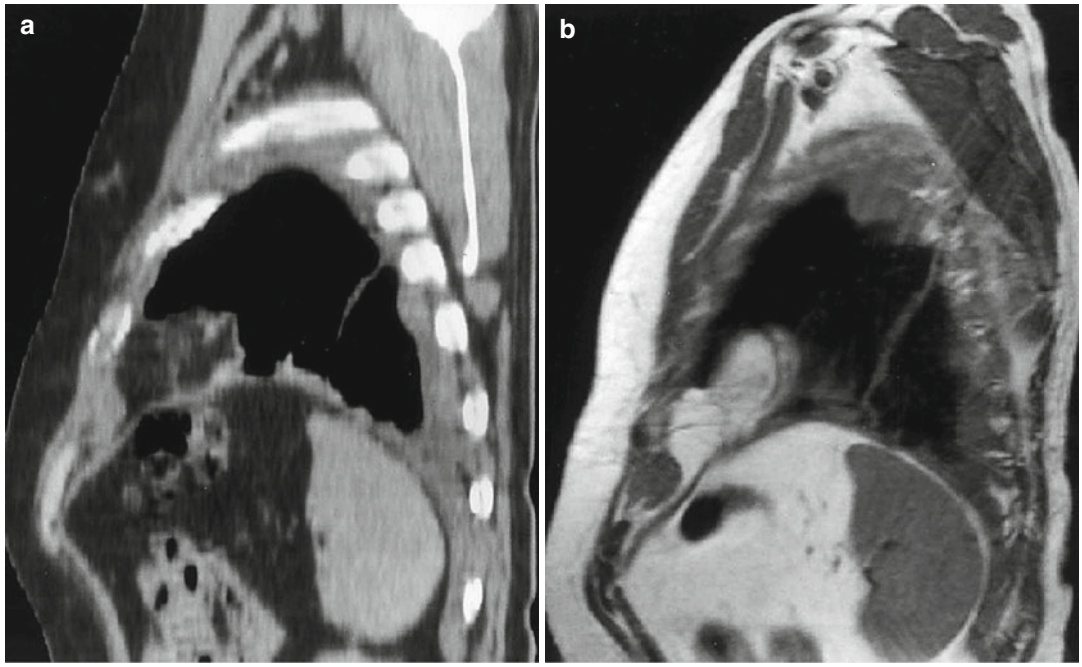

Fig. 17.15 Resectable MPM (T3). Reconstructed sagittal CT image (**a**) and sagittal T1-weighted MRI scan (**b**) show an irregular pleural thickening with tumor spreading into the fissure and involvement of the left hemidiaphragm without evidence of transdiaphragmatic extent. The abdominal surface of the diaphragm is smooth, and a clear fat plane is seen between diaphragm and spleen

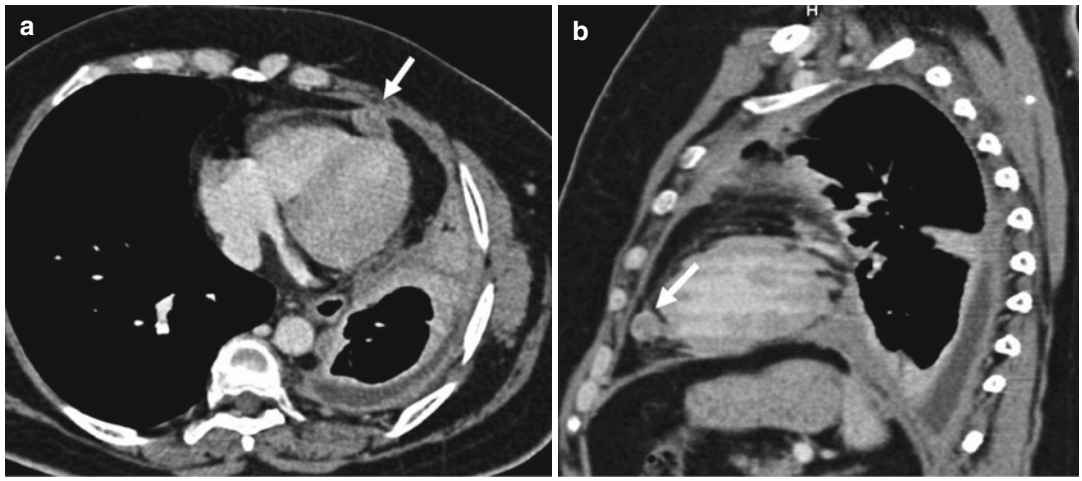

Fig. 17.16 Sixty-two-year-old woman with T4 unresectable MPM. There is a left-sided MPM typically determined by volume loss, pleural thickening, and pleural effusion. Notice the presence of a tumoral nodule along the internal surface of the pericardium (*arrows* in **a** and **b**) with focal obliteration of the pericardial fat caused by this unresectable tumor

with an allergy to contrast material or to confirm or support suspicion of involvement of anatomic structures revealed by CT.

Little information is available about diagnosis by CT and MRI of nodal (N1–N3) involvement in MPM. Therefore, two factors may render

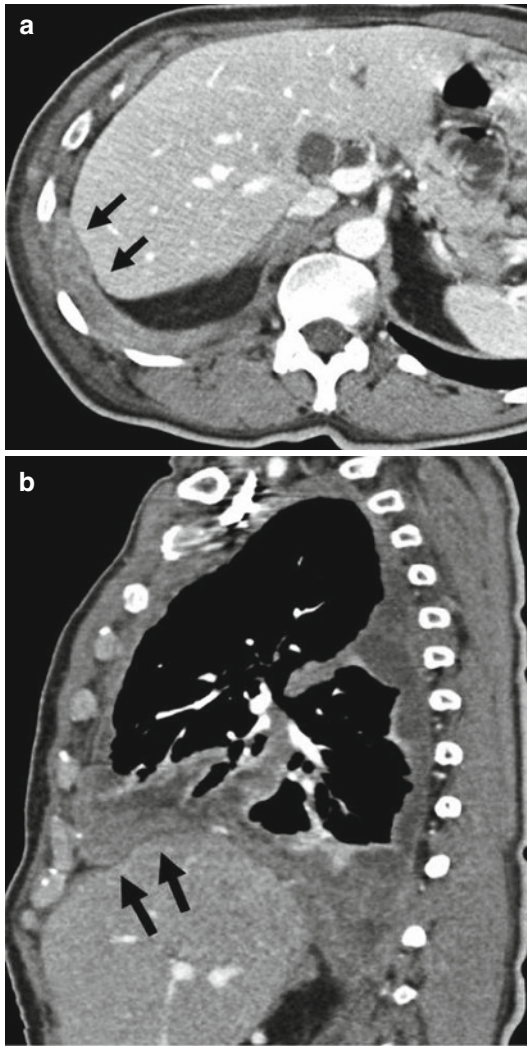

Fig. 17.17 Non-resectable MPM (T4). Axial (**a**) and sagittal reconstructed (**b**) CT images demonstrate transdiaphragmatic invasion of the tumor as shown by the obliteration of the abdominal fat and the irregular interface between the tumor and the liver (*arrows* in **a** and **b**)

imaging diagnosis of N disease difficult: involved nodes may not be enlarged, and large portions of the ipsilateral hilum and mediastinum may be obscured by bulky sheets of locally invasive or adjacent tumor (Patz et al. 1996; Heelan et al. 1999). Mediastinal, hilar, and abdominal lymph nodes should be considered abnormal if greater than 1 cm in short axis, internal mammary lymph nodes if larger than the accompanying vessels, and cardiophrenic lymph nodes if greater than 5 mm in short axis. Retropleural lymph nodes should always be considered involved independently of their size (Seely et al. 2009).

No TNM staging system fully recognizes the pathologic and biologic variables that influence survival. Many factors are reported to be prognostic in MPM, including histology, age, sex, performance status, type of symptoms, weight loss, history of asbestos exposure, and platelet count (Baas et al. 1998; Boutin et al. 1993; Sugarbaker et al. 1999; Rusch and Venkatraman 1996; Curran et al. 1998; De Prangher Manzini et al. 1993; Van Gelder et al. 1994). Of these, only histology appears to be universally accepted, with all of the studies finding that epithelioid mesothelioma is always associated with a significantly better outcome than the sarcomatoid or mixed variants. Although the TNM staging system provides an accurate description of tumor extension, it does not recognize its histological variant; because of the aggressiveness of sarcomatoid mesothelioma, this form is not surgically removed even when technically respectable (T3).

17.2.1.2 Localized Fibrous Tumor

Localized fibrous tumor is a relatively uncommon mesenchymal neoplasm which usually involves the pleura, but it can occur in other thoracic areas (mediastinum, pericardium, and lung) as well as in extrathoracic areas (meninx, epiglottis, salivary glands, thyroid, kidneys, and breast). This tumor accounts for about 10 % of primary tumors of the pleura. It has been described in all age groups but has a peak incidence in the fourth, fifth, and sixth decades of life, without any gender predilection. Unlike MPM, this tumor is not related to asbestos exposure (England et al. 1989). About 80 % of localized fibrous tumors arise from the visceral pleura and the remaining 20 % from the parietal pleura; an origin from within a fissure is fairly common. Although they are often referred to as "localized, fibrous, or benign mesotheliomas," this terminology is inappropriate because fibrous tumors are believed to originate from submesothelial mesenchymal cells rather than from the mesothelial lining cells, and moreover, they exist in benign and malignant forms. Varying percentages from 12 to 37 % of localized

fibrous tumors are histologically malignant (England et al. 1989). The distinction between benign and malignant forms can be made on histologic ground, but is often difficult; the presence of a pedicle is the best evidence of benignity. This sign is present in about 50 % and the stalk can be up to 9 cm in length. About half of the patients are asymptomatic, and the tumor is usually detected incidentally at chest radiography. Otherwise, the usual symptoms are cough, chest pain, and dyspnea. These tumors have traditionally been considered to have a high incidence of paraneoplastic manifestations such as hypertrophic pulmonary osteoarthropathy, seen in about 35 % of the patients (Briselli et al. 1981).

Histologically, the lesions are usually composed of spindle-shaped cells similar to fibroblasts contained within a stroma of collagenous fibers. Hypercellular areas may alternate with hypocellular fibrous areas, hemorrhagic, myxoid, or necrotic areas (Briselli et al. 1981). Tumor cells are immunoreactive for CD34 and CD99; usually cytokeratins and desmin are negative. Macroscopically, the tumor is seen as a circumscribed, spherical, or ovoid mass that arises in the pleural space, usually solitary, ranging in size from less than 1–30 cm; calcifications are present in only 5 % of cases.

Preoperative diagnosis can be obtained by a transthoracic cutting needle biopsy, but in most cases, only pathological evaluation of the resected specimen supported by immunoreactivity of neoplastic cells for CD34 or CD99 allows confirmatory diagnosis.

Radiological Features

Radiologically, the usual finding is a rounded or oval, often lobulated, homogeneous mass abutting the pleural surface. The tumor displays the signs commonly seen in extraparenchymal lesions (Fig. 17.18), such as an incomplete visualization of the lesion margins and the sharp delineation of the mass on tangential views. Another common finding in pleural lesions, the obtuse angles formed between the mass and the chest wall or mediastinum, is seen in 74–94 % of the cases and is better seen in small lesions. The largest dimension is generally in the longitudinal plane. The mass is slightly more common in the lower half of the chest with no predilection for either side; it is seen along the chest wall pleura in 46 % of cases, within an interlobar fissure in 30 %, abutting the mediastinal pleura in 18 % and contiguous to the diaphragm in 6 %. The tendency for these tumors to change position with respiration or posture may be helpful for the diagnosis (Dedrick et al. 1985). At CT imaging, localized fibrous tumor usually appears as a well-defined, smoothly marginated lobular pleural mass of varying density which is homogeneous in small lesions and inhomogeneous in large lesions as a result of necrosis or myxoid degeneration or hemorrhage (Lee et al. 1992; Cardinale et al. 2010). Calcifications are rare and associated pleural effusion is sometimes seen (17 %). The CT pattern is certainly not characteristic; nonetheless, a "gradually tapering" interface between mass and chest wall (Fig. 17.18) and displacement of adjacent lung parenchyma with compressive atelectasis and bowing of the bronchi and pulmonary vessels around the mass appear to be a reliable sign of the pleural origin of the mass. In large tumors, pleural localization may be suspected based on the position of the mass, which is usually oriented longitudinally. Tumors located within the fissural space may be interpreted as pulmonary masses when they appear totally surrounded by pulmonary parenchyma; use of thin-slice multidetector CT with multiplanar reconstructions allows better visualization of the fissure and its relationship with the tumor. Likewise, CT findings of fissural tails with obtuse tumor-fissure angles and a lentiform shape of tumor could correctly indicate a fissure-originated tumor. Fibrous tumors that have a mediastinic pleural origin can mimic a mediastinal neoplasm, and differential diagnosis may be very difficult; also in these cases, a careful analysis of multiplanar and volumetric reformatted CT images is crucial. In fact lesions of pleural origin typically determine compression and dislocation of the mediastinum, contrary to what occurs in the presence of a mediastinal mass which expands compressing the pulmonary parenchyma without causing mediastinal shift.

Pedunculated pleural fibromas can be diagnosed when changes in lesion position and shape are detected between scans performed with the patient supine and additional scans with the patient in the prone position. After intravascular contrast

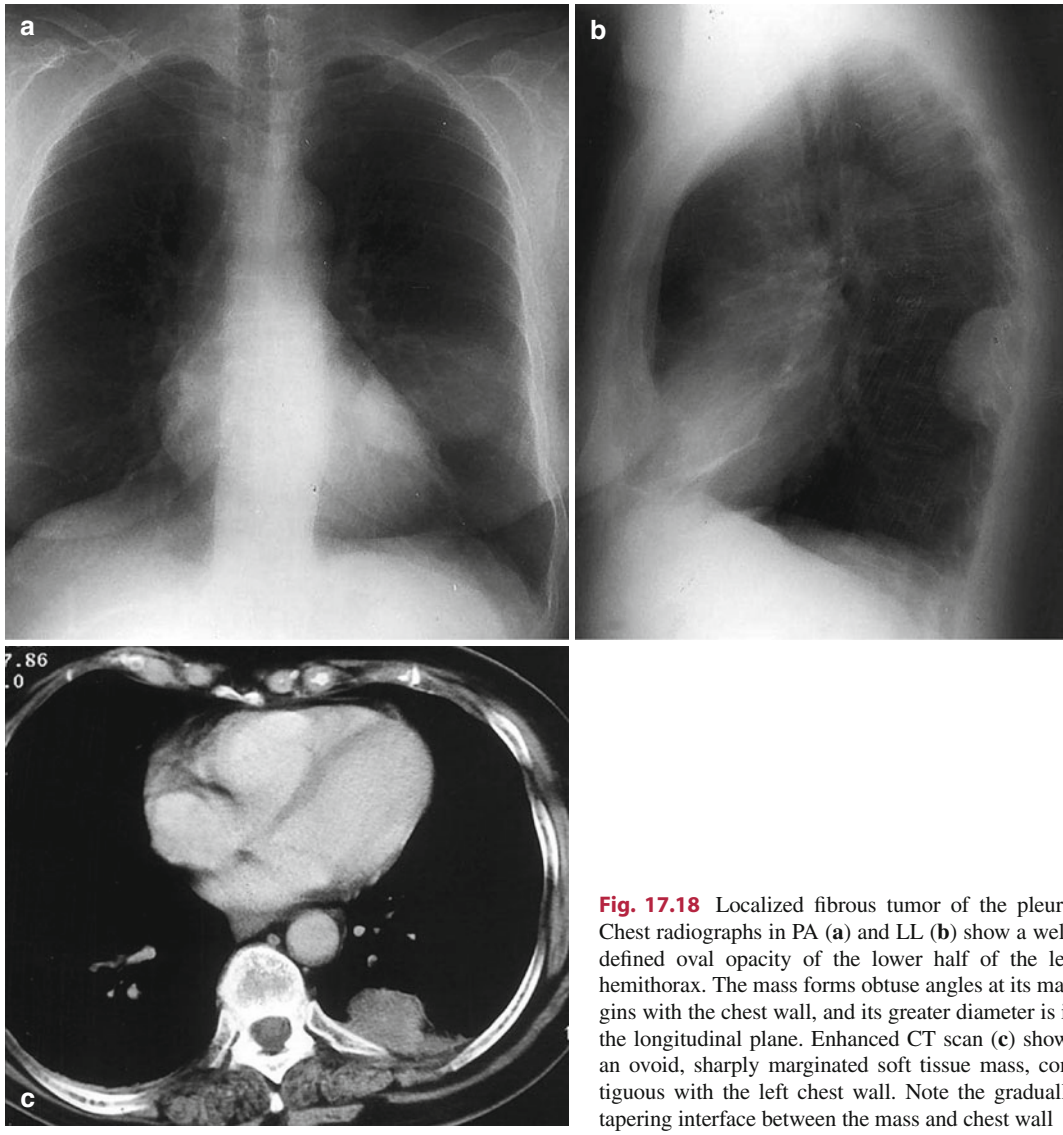

Fig. 17.18 Localized fibrous tumor of the pleura. Chest radiographs in PA (**a**) and LL (**b**) show a well-defined oval opacity of the lower half of the left hemithorax. The mass forms obtuse angles at its margins with the chest wall, and its greater diameter is in the longitudinal plane. Enhanced CT scan (**c**) shows an ovoid, sharply marginated soft tissue mass, contiguous with the left chest wall. Note the gradually tapering interface between the mass and chest wall

material, enhancement is variable; generally, it is equal to or greater than that of other soft tissues in all patients and can be inhomogeneous especially in large tumors (Mendelson et al. 1991). On MRI, localized fibrous tumors appear hypointense on T1-weighted sequences, whereas they display inhomogeneous and variable intensity as they may be hypo-, iso-, or hyperintense relative to the chest wall musculature. These signal characteristics reflect the high cellularity and the typical histological heterogeneity of the tumor; when they are predominantly composed of fibrous tissue, on T2-weighted sequences they appear hypointense to muscles with the presence of foci of hyperintensity (Dynes et al. 1992).

Prognosis of localized fibrous tumors is generally good even though 15 % of cases recur after surgical resection.

17.2.1.3 Pleural Sarcoma

Sarcomas constitute very rare pleural tumors which include several histological types: liposarcoma, chondrosarcoma, osteosarcoma, and malignant schwannoma; cases of pleural synovial sarcoma have also been reported (Munk and Müller 1988). They are very aggressive tumors that arise from pluripotent mesenchymal cells and tend to affect young adults between 20 and 40 years. Their radiological patterns vary depending on their histological features; in particular, liposarcomas show areas of dishomogeneous fat density (with attenuation values generally lower than 50 HU) (Fig. 17.19), whereas chondrosarcomas and osteosarcomas frequently contain calcifications (Evans et al. 1985). These tumors have a tendency to massively infiltrate the chest wall, and they often spread to extrathoracic sites.

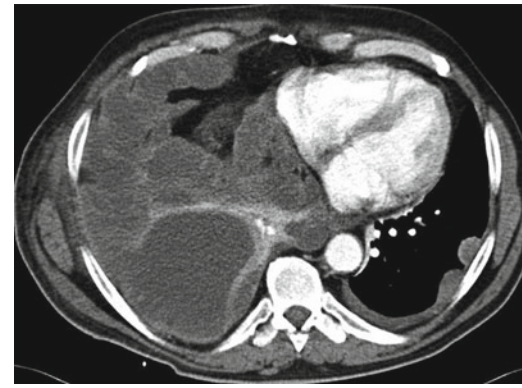

Fig. 17.19 Right pleural liposarcoma. CT image displays multiloculated pleural masses with areas of inhomogeneous fat density infiltrating the mediastinum and the chest wall; pleural effusion and pleural metastases are also seen on the left hemithorax

17.2.2 Secondary Tumors

17.2.2.1 Pleural Metastases

The most common finding in patients with pleural metastases is pleural effusion; in a review of 1.783 cases of malignant pleural effusions, bronchogenic carcinoma, especially adenocarcinoma, accounted for 36 %, breast cancer for 25 %, lymphoma for 10 %, and ovarian and gastric carcinoma for 5 % or less (Sahn 1988b). In approximately 7 % of patients with malignant pleural effusion, the primary site is unknown when the diagnosis is first established (Table 17.2). Among the causes of pleural effusion in patients over 50 years, pleural metastases are second only to congestive heart failure. The main cause for the effusion is thought to be an impairment in lymphatic drainage anywhere between the parietal pleura and the mediastinal lymph nodes (Sahn 1988b; Müller 1993); in addition, the presence of tumor results in increased capillary permeability due to inflammation, infiltration of tumor cells, and/or obstruction of venules (Matthay et al. 1990; DeCamp et al. 1997). The exudate related to malignant disease is characterized by increased protein concentration (>2 g/dl) and by lymphocytosis (50–70 %), predominantly supported by T lymphocytes that appear to play a role in the local defense against tumor invasion of the pleural cavity. Other frequent findings are increased LDH and hyaluronic acid; the percentage of mesothelial cells is variable. In 30 % of cases, the pH is low (<7.30), as is the glucose level (<60 mg/dl); this usually occurs in diffuse pleural tumors as glucose is also metabolized by the tumor cells with production of lactate and CO_2. The tumor-induced alterations in pleural permeability prevent outflow of the glucose metabolism products resulting in acidosis. Finally, in adenocarcinoma metastases, the CEA levels may be elevated, although this is a nonspecific finding also seen in several benign conditions such as empyema, tuberculosis, pancreatitis, and cirrhosis.

Table 17.2 Causes of malignant pleural effusions

Tumor	%
Lung	36
Breast	25
Lymphoma	10
Ovary	5
Stomach	2
Unknown primary	7
Other causes	14

Although pleural effusion is often the major component of metastatic disease to the pleura, other findings include pleural nodules or extensive

pleural thickening. Metastatic pleural lesions may also appear as a solitary implant on the costal, diaphragmatic, or mediastinal pleura or within the interlobar fissures (Sahn 1997).

The tumor cells reach pleural surfaces via the blood, the lymph, or by contiguity with different mechanisms depending on whether the primary tumor is intra- or extrathoracic.

Hematogenous spread to the pleura of intrathoracic tumors, in particular pulmonary adenocarcinoma, is often monolateral located ipsilaterally to the primary tumor; this occurs as a result of tumor emboli reaching the visceral pleura via the pulmonary artery with subsequent invasion of the parietal pleura through pleural adhesions or attachment of exfoliated tumor cells. Bilateral pleural involvement, by contrast, is usually associated with liver metastases, independent of the intra- or extrathoracic origin of the primary tumor; pleural metastases result from the hematogenous spread of the tumor cells directly from the liver to the parietal pleura which is supplied by vessels from the systemic circulation (Meyer 1966).

Lymphatic spread from intra- or extrathoracic tumors is not rare; in particular tumors located in the abdominal cavity may spread to the pleura even via transdiaphragmatic lymph vessels. In other cases, the tumors metastasize to the pleura via direct infiltration; this may occur with intrathoracic lesions such as lung (especially adenocarcinoma) or breast cancers, but rarely with subdiaphragmatic cancers (gastric, pancreatic, liver cancers).

Imaging modalities may suggest the diagnosis of secondary pleural localizations in the presence of known primary tumors; however, in many cases, the final diagnosis requires the use of more invasive methods, such as pleural fluid cytology, pleural biopsy, or thoracotomic exploration. The radiological appearance of pleural metastases is very similar to that of other pleural malignancies appearing as nodular pleural thickening often associated to mono or bilateral pleural effusion. In patients with unilateral metastasis to the pleura, the radiologic findings may be indistinguishable from those of mesothelioma. Clearly, neither CT nor MRI is capable of suggesting the site of primary tumor on the basis of morphological features of pleural lesions; nonetheless, some particular aspects should be recalled that may be helpful for the diagnosis: metastases from breast and ovarian cancer and from osteosarcoma tend to show calcifications (50–70 %) unlike those from other cancers. The calcifications may appear after treatment with chemotherapy, above all in ovarian cancer. In other cases, the metastases may display an unusual appearance in that they present as multiple nodular masses with intense peripheral rim enhancement after contrast administration.

Bronchogenic carcinoma, above all adenocarcinoma, represents the most frequent cause of pleural malignancy. The presence of secondary pleural involvement considerably affects the staging, prognosis, and treatment of the disease (Detterbeck et al. 2009). A bronchogenic carcinoma invading the visceral pleura is classified as a T2 lesion, while extension into the mediastinal pleura or parietal pleura changes the classification to T3. Neither case prevents surgical resection. Tumors with pleural nodules or cytologically malignant pleural effusion are classified as M1a and, therefore, are unresectable. A benign reactive cytologically negative pleural effusion has no staging significance. CT has poor predictive value in distinguishing contiguity of the neoplasm with the pleural surface from pleural, mediastinal, or chest wall invasion (Glazer et al. 1985; Scott et al. 1988; Yokoi et al. 1991). Contact of tumor with the pleural surface, angle between tumor and pleura, pleural thickening, and pleural effusion have a low specificity in the detection of pleural invasion. MRI is superior to CT in the evaluation of parietal pleural and chest wall invasion. Focal parietal tumoral signal intensity with T1-weighted sequences is the most sensitive and specific sign of parietal invasion (Schmutz et al. 1993). MRI may also contribute to the evaluation of superior sulcus tumors and peridiaphragmatic tumors, especially with the use of coronal and sagittal planes (Shuman and Libshitz 1984).

17.2.2.2 Pleural Lymphoma

It has been estimated that approximately 10 % of malignant pleural effusions are the result of lymphoma (Sahn 1988b).

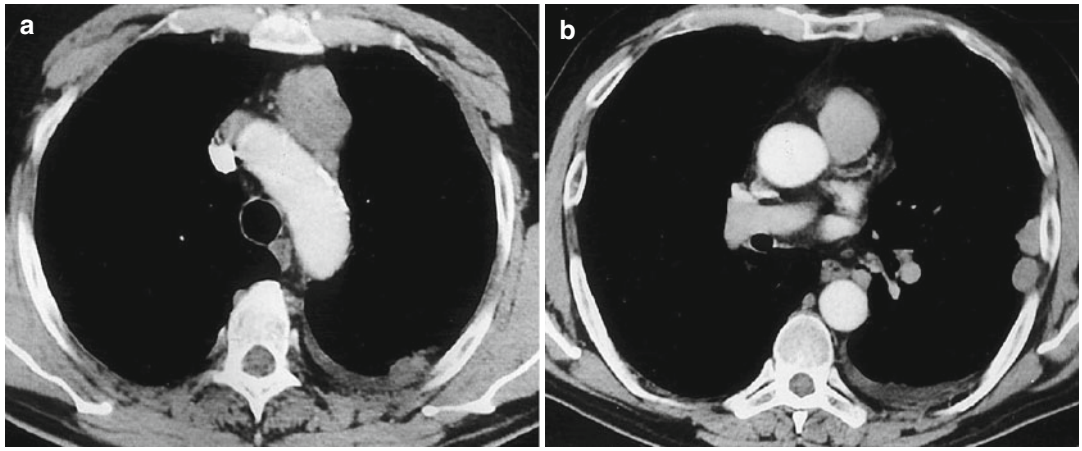

Fig. 17.20 Invasive thymoma. Enhanced CT scan, obtained through the aortic arch (**a**), demonstrates a solid anterior mediastinal mass and pleural seeding with distant implants. There is associated pleural effusion. CT scan obtained at a lower level (**b**) shows pleural-based tumor nodules along the left parietal pleura

Involvement of the pleura by lymphoma may occur in both Hodgkin (11.4–30 %) and non-Hodgkin disease (3.7–33 %) (Schmutz et al. 1993). Pleural lymphoma represents either a site of recurrence or an extension of the disease from mediastinal and/or pulmonary lymphoma (Malatskey et al. 1989). Pleural lymphoma presenting as the initial manifestation of the disease is rare (Carlson et al. 1993). On CT and MRI, pleural lymphoma appears either as a solitary nodule or as multiple, broad-based pleural plaques usually associated with pleural effusion (Carlson et al. 1993). While pleural effusion in lymphoma can be due either to obstruction of lymphatic drainage by mediastinal lymphadenopathy, to pleural infiltration, or to thoracic duct obstruction, impaired lymphatic drainage appears to be the primary mechanism in Hodgkin disease and direct pleural infiltration the predominant cause in non-Hodgkin lymphoma (Sahn 1997). Nodules represent the confluence of lymphoid tissue; the lymphomatous deposits arise from lymphatic channels and lymphoid aggregates in the subpleural connective tissue below the visceral pleura. True visceral pleural invasion is uncommon. Nodules may also occur in pleural fissures. The detection of noncontiguous additional pleural involvement changes the classification particularly in Hodgkin disease and may alter the therapeutic plan. Shuman and Libshitz have documented a role of CT in detecting pleural involvement (Shuman and Libshitz 1984). In a series of 71 patients with both documented Hodgkin ($n=47$) and non-Hodgkin lymphoma ($n=24$) evaluated by CT, these authors showed solid pleural manifestations in 31 % of cases. Although this most probably does not represent typical populations of patients, as pointed out by the authors themselves, it is clear that, when staging lymphoma patients, the search for possible pleural metastases should not be overlooked. The treatment of lymphoma may change the appearance of the nodules and plaques which may become calcific or cystic.

17.2.2.3 Invasive Thymoma

Invasive thymoma metastasizes to the pleura by indirect invasion of tumor cells or by "drop metastasis." Pleural implants from mediastinal thymoma may appear even years after removal of the primary tumor resulting, on CT and/or MRI, in either widespread pleural thickening or multiple circumscribed masses (Fig. 17.20). When the anterior mediastinal tumor component of the thymoma is small, the distinction from a malignant pleural mass is difficult. At CT thymoma appears as an asymmetric homogeneous soft tissue mass with moderate enhancement after contrast injection. On T1-weighted sequences thymoma appears homogeneous and isointense to skeletal

muscle, while on T2-weighted images, the mass has a signal intensity approaching that of fat and appears inhomogeneous. Invasive thymoma grows through its capsule into the mediastinum with encasement of local vessels along the pleural and pericardial surfaces; it may spread through the diaphragm into the liver and the retroperitoneal space (Scatariage et al. 1985; Zerhouni et al. 1982). Pleural seeding often occurs as recurrent disease after surgery, and therefore, CT or MRI is recommended in the follow-up of patients with a history of surgery or radiation therapy.

References

Abdel Rahman AR, Gaafar RM, Baki HA, El Hosieny HM, Aboulkasem F, Farahat EG, Nouh AM, Mansour KA (2008) Prevalence and pattern of lymph node metastasis in malignant pleural mesothelioma. Ann Thorac Surg 86:391–395

Aberle DR, Barnes JR (1991) Computerized tomography of asbestos-related pulmonary parenchymal and pleural disease. Clin Chest Med 12:115–131

Antman KH (1980) Malignant mesothelioma. N Engl J Med 303:200–202

Baas P, Schouwink H, Zoetmulder FAN (1998) Malignant pleural mesothelioma. Ann Oncol 9:139–149

Boutin C, Rey F (1993) Thoracoscopy in pleural malignant mesothelioma: a prospective study of 188 consecutive patients. I. Diagnosis. Cancer 72:389–393

Boutin C, Rey F, Gouvernet J, Viallat JR, Astoul P, Ledoray V (1993) Thoracoscopy in pleural malignant mesothelioma: a prospective study of 188 consecutive patients. II. Prognosis and staging. Cancer 72: 394–404

Briselli M, Mark EJ, Dickersin GR (1981) Solitary fibrous tumor of the pleura: eight new cases and review of 360 cases in the literature. Cancer 47:2678–2689

Butchart EG, Ashcroft T, Barnsley WC, Holden MP (1976) Pleuropneumonectomy in the management of diffuse malignant mesothelioma of the pleura: experience with 29 patients. Thorax 31:15–24

Carbone M, Rizzo P, Grimley PM et al (1997) Simian virus-40-large-T antigen binds p53 in human mesotheliomas. Nat Med 3:908–913

Cardinale L, Ardissone F, Volpicelli G, Solitro F, Fava C (2010) CT signs, patterns and differential diagnosis of solitary fibrous tumors of the pleura. J Thorac Dis 2:21–25

Carlson SE, Bergin CJ, Hoppe RT (1993) MR imaging to detect chest wall and pleural involvement in patients with lymphoma: effect on radiation therapy planning. AJR Am J Roentgenol 160:1191–1195

Churg A (1988) Chrysotile, tremolite and malignant mesothelioma in man. Chest 93:621–628

Craighead JE, Abraham JL, Churg A et al (1982) The pathology of asbestos-associated diseases of the lungs and pleural cavities: diagnostic criteria and proposed grading schema. Arch Pathol Lab Med 106:544–597

Curran D, Sahmoud T, Therasse P, van Meerbeeck J, Postmus PE, Giaccone G (1998) Prognostic factors in patients with pleural mesothelioma: the European organization for research and treatment of cancer experience. J Clin Oncol 16(1):145–152

Damhuis RAM, Planteydt HT (1995) Trends in incidence of pleural mesothelioma in the Rotterdam area. Int J Cancer 60:883

De Prangher Manzini V, Brollo A, Franceschi S et al (1993) Prognostic factors of malignant mesothelioma of the pleura. Cancer 72:410–417

DeCamp MM, Mentzer SJ, Swanson SJ, Sugarbaker DJ (1997) Malignant effusive disease of the pleura and pericardium. Chest 112:291S–295S

Dedrick CJ, McCloud TC, Shepard JO, Shipley RT (1985) Computerized tomography of localized pleural mesothelioma. AJR Am J Roentgenol 144:275–280

Detterbeck FC, Boffa DJ, Tanoue LT (2009) The New lung cancer staging system. Chest 136:260–271

Dynes MC, White EM, Fry WA, Ghahremani GG (1992) Imaging manifestations of pleural tumors. Radiographics 12:1191–1201

England DM, Hochholzer L, McCarthy MJ (1989) Localized benign and malignant fibrous tumors of the pleura: a clinicopathologic review of 223 cases. Am J Surg Pathol 13:640–658

Evans AR, Wolstenholte RJ, Shettar SP, Yogish H (1985) Primary pleural liposarcoma. Thorax 40:554–555

Falaschi F, Battolla L, Mascalchi M, Cioni R, Zampa V, Lencioni R, Antonelli A, Bartolozzi C (1996) Usefulness of MR signal intensity in distinguishing benign from malignant pleural disease. AJR 166: 963–968

Feragalli B et al. (2003): Malignant Pleural disease. Radiol Med.105(4):266–288

Fraire AE, Cooper S, Greenberg SD, Buffler P, Langston C (1988) Mesothelioma of childhood. Cancer 62: 838–847

Gallardo X, Castaner E, Mata JM (2000) Benign pleural diseases. Eur J Radiol 34:87–97

Gilbert TB (1993): Hemodynamic consequences of tension pneumothorax. Crit Care Med 21(12):1981–1982

Glazer HS, Duncan-Meyer J, Aronberg DJ, Moran JF, Levitt RG, Sagell SS (1985) Pleural and chest wall invasion in bronchogenic carcinoma: CT evaluation. Radiology 157:191–194

Greenberg D (1992) Benign asbestos-related pleural diseases. In: Roggli VL, Greenberg SD, Pratt PC (eds) Pathology of asbestos-associated diseases. Little, Brown, New York, pp 165–187

Hammar SP (1994a) Pleural diseases. In: Dail DH, Hammar SP (eds) Pulmonary pathology, 2nd edn. Springer, New York, pp 1487–1553

Hammar SP (1994b) The pathology of benign and malignant pleural disease. Chest Surg Clin N Am 4(3): 405–430

Hammar SP, Bockus D, Remington F, Friedman S, LaZerte G (1989) Familiar mesothelioma: a report of two families. Hum Pathol 20:107–112

Heelan RT, Rusch VW, Begg CB, Panicek DM, Caravelli JF, Eisen C (1999) Staging of malignant pleural mesothelioma: comparison of CT and MR imaging. AJR Am J Roentgenol 172:1039–1047

Hierholzer J, Luo L, Bittner LC, Stroszczynski C, Schröder R-J, Schoenfeld N, Dorow P, Loddenkemper R, Grassot A (2000) MRI and CT in the differential diagnosis of pleural disease. Chest 118:604–609

Hillerdal G (1994) Pleural plaques and risk for bronchial carcinoma and mesothelioma: a prospective study. Chest 105:144–150

Hillerdal G, Berg J (1985) Malignant mesothelioma secondary to chronic inflammation and old scars: two new cases and review of the literature. Cancer 55:1968–1972

Hulnick DH, Naidich DP, Mc Cauley DI (1983) Pleural tuberculosis evaluated by computed tomography. Radiology 149:759–765

Huncharek M (1992) Changing risk groups for malignant mesothelioma. Cancer 69:2704–2711

Huncharek M (1994) Miliary mesothelioma. Chest 106: 605–606

Huncharek M, Smith K (1988) Extrathoracic lymph node metastases in malignant pleural mesothelioma (letter). Chest 93:443–444

International Mesothelioma Interest Group (1995) A proposed new international TNM staging system for malignant pleural mesothelioma. Chest 108:1122–1128

Kane MJ, Chahinian AP, Holland JF (1990) Malignant mesothelioma in young adults. Cancer 65:1449–1455

Kawashima A, Libshitz HI (1990) Malignant pleural mesothelioma: CT manifestations in 50 cases. AJR Am J Roentgenol 155:965–969

Lee KS, Im JG, Choe KO, Kim CJ, Lee BH (1992) CT findings in benign fibrous mesothelioma of the pleura: pathologic correlation in nine patients. AJR Am J Roentgenol 158:983–986

Leung AN, Müller NL, Miller RR (1990) CT in differential diagnosis of diffuse pleural disease. AJR AmJ Roentgenol 154:487–492

Light RW (1990) Diseases of the pleura, mediastinum, chest wall, and diaphragm. In: George RB, Light RW, Matthay MA, Matthay RA (eds) Chest medicine. Williams & Wilkins, Baltimore, pp 381–412

Malatskey A, Fields S, Libson E (1989) CT appearance of primary pleural lymphoma. Comput Med Imaging Graphics 13:165–167

Matthay RA, Coppage L, Shaw C, Filderman AE (1990) Malignancies metastatic to the pleura. Invest Radiol 25:601–619

McDonald AD, McDonald JC (1980) Malignant mesothelioma in North America. Cancer 46:1650–1656

McLoud TC, Flower CDR (1991a) Imaging the pleura: sonography, CT and MR imaging. Am J Roentgenol 156:1145–1153

McLoud TC, Flower CDR (1991b) Imaging of the pleura: sonography. CT and MR imaging. AJR Am J Roentgenol 156:1145–1153

Mendelson DS, Meary E, Buy JN, Pigeau I, Kirschner PA (1991) Localized fibrous pleural mesothelioma: CT findings. Clin Imaging 15:105–108

Meyer PC (1966) Metastatic carcinoma of the pleura. Thorax 21:437–443

Miller BH, Rosado-de-Christenson ML, Mason AC, Fleming MV, White CC, Krasna MJ (1996) Malignant pleural mesothelioma: radiologic-pathologic correlation. Radiographics 16:613–644

Montalvo BM, Morillo G, Sridhar K, Christoph C (1991) MR imaging of malignant pleural mesothelioma. Abs. Radiology 181(P):109

Moskowitz H, Platt RT, Schachar R, Mellins H (1973) Roentgen visualization of minute pleural effusion. Radiology 109:33–35

Mossman BT, Churg A (1998) Mechanism in pathogenesis of asbestosis and silicosis. Am J Respir Crit Care Med 157:1666–1680

Muller NL (1993) Imaging of the pleura. Radiology 186: 297–309

Müller NL (1993) Imaging of the pleura. Radiology 186: 297–309

Munk PL, Müller NL (1988) Pleural liposarcoma. CT diagnosis. J Comput Assist Tomogr 12:709–710

O'Moore PV, Mueller PR, Simeone JF et al (1987) Sonographic guidance in diagnostic and therapeutic interventions in the pleural space. Am J Roentgenol 149:1–5

Pass HI (1994) Contemporary approaches in the investigation and treatment of malignant pleural mesothelioma. Chest Surg Clin N Am 4:497–515

Patz EF, Shaffer K, Piwnica-Worms DR, Jochelson M, Sarin M, Sugarbaker DJ, Pugatch RD (1992) Malignant pleural mesothelioma: value of CT and RM imaging in predicting resectability. AJR Am J Roentgenol 159:961–966

Patz EF, Rusch VW, Heelan R (1996) The proposed new international TNM staging system for malignant pleural mesothelioma: application to imaging. AJR Am J Roentgenol 166:323–327

Peterson JT Jr, Greenberg SD, Buffler PA (1984) Non-asbestos-related malignant mesothelioma: a review. Cancer 54:951–960

Peto J, Hodgson JT, Matthews FE, Jones JR (1995) Continuing increase in mesothelioma mortality in Britain. Lancet 345:535–539

Pisani RJ, Colby TV, Williams DE (1988) Malignant mesothelioma of the pleura. Mayo Clin Proc 63:1234–1244

Pistolesi M, Miniati M, Giuntini C (1989) State of the art: pleural liquid and solute exchange. Am Rev Respir Dis 140:825–847

Roggli VL, Sanfilippo F, Shelburne JD (1992) Mesothelioma. In: Roggli VL, Greenberg SD, Pratt PC (eds) Pathology of asbestos-associated diseases. Little, Brown, New York, pp 109–153

Rudd RM (1996) New developments in asbestos-related pleural disease. Thorax 51:210–216

Ruffie P (1992) Pleural mesothelioma. Curr Opin Oncol 4:334–341

Rusch VW, Venkatraman E (1996) The importance of surgical staging in the treatment of malignant pleural mesothelioma. J Thorac Cardiovasc Surg 111:815–826

Sahin AA, Çöplü L, Selçuk ZT, Eryilmaz M, Emri S, Akhan O, Baris YI (1993) Malignant pleural mesothelioma caused by environmental exposure to asbestos or erionite in rural Turkey: CT findings in 84 patients. AJR 161:533–537

Sahn SA (1988a) State of the art: the pleura. Am Rev Respir Dis 138:184–234

Sahn SA (1988b) Malignant pleural effusion. In: Fishman AP (ed) Pulmonary diseases and disorders, 2nd edn. McGraw-Hill, New York, pp 2159–2169

Sahn SA (1997) Pleural disease related to metastatic malignances. Eur Respir J 10:1907–1913

Scatariage JC, Fishman EK, Zerhouni EA et al (1985) Transdiaphragmatic extension of invasive thymoma. AJR Am J Roentgenol 144:31–35

Schmutz GR, Fisch-Ponsot C, Regent D, Sylvestre J (1993) CT and MRI of pleural masses. Crit Rev Diagn Imag 34(6):309–383

Scott IR, Müller NL, Miller RR, Evans KG, Nelems B (1988) Resectable stage III lung cancer: CT, surgical and pathologic correlation. Radiology 166:75–79

Seely JM, Nguyen ET, Churg AM, Müller NL (2009) Malignant pleural mesothelioma: computed tomography and correlation with histology. Eur J Radiol 70(3):485–491

Selikoff IJ, Hammond EC, Seidman H (1980) Latency of asbestos disease among insulation workers in the United States and Canada. Cancer 46:2736–2740

Shuman LS, Libshitz HI (1984) Solid pleural manifestations of lymphoma. AJR Am J Roentgenol 142:269–273

Silverman SG, Mueller PR, Saini S et al (1988) Thoracic empyema: management with image-guided catheter drainage. Radiology 169:5–9

Staub NC, Wiener-Kronish JP, Albertine KH (1985) Transport through the pleura: physiology of normal liquid and solute exchange in the pleural space. In: Chretien J, Bignon J, Hirsch A (eds) The pleura in health and disease. Marcel Dekker, New York, pp 169–193

Sugarbaker DJ, Heher EC, Lee TH, Couper G, Mentzer S, Corson JM, Collins JJ, Shemin R, Pugatch R, Weissman L, Antman KH (1991) Extrapleural pneumonectomy, chemotherapy and radiotherapy in the treatment of diffuse malignant pleural mesothelioma. J Thorac Cardiovasc Surg 102:10–15

Sugarbaker DJ, Strauss GM, Lynch TJ, Richards W, Mentzer SJ, Lee TH et al (1993) Node staging has prognostic significance in the multimodality therapy of diffuse malignant mesothelioma. J Clin Oncol 11: 1172–1178

Sugarbaker DJ, Flores RM, Jaklitsch MT, Richards WG, Strauss GM, Corson JM, DeCamp MM, Swanson SJ, Bueno R, Lukanich JM, Baldini EH, Mentzer SJ (1999) Resection margins, extrapleural nodal status and cell type determine postoperative long-term survival in trimodality therapy of malignant pleural mesothelioma: results in 183 patients. J Thorac Cardiovasc Surg 117:54–65

Tocino IM, Miller MH, Fairfax WR (1985) Distribution of pneumothorax in the supine and semirecumbent critically ill adult. Am J Roentgenol 144:901

Van Gelder T, Damhuis RA, Hoogsteden HC (1994) Prognostic factors and survival in malignant pleural mesothelioma. Eur Respir J 7:1035–1038

Wagner JC, Sleggs CA, Marchand P (1960) Diffuse pleural mesothelioma and asbestos exposure in Northwestern Cape Province. Br J Ind Med 17: 260–271

Wechsler RJ, Rao VM, Steiner RM (1983) The radiology of thoracic malignant mesothelioma. Crit Rev Diagn Imaging 20:283–310

Wick MR, Loy T, Mills SE, Legier JF, Manivel JC (1990) Malignant epithelioid pleural mesothelioma versus peripheral pulmonary adenocarcinoma: a histochemical, ultrastructural and immunohistologic study of 103 cases. Hum Pathol 21:759–766

Williford ME, Godwin JD (1983) Computed tomography of lung abscess and empyema. Radiol Clin North Am 21:575–583

Yang PC, Luh KT, Chang DB, Wu HD, Yu CJ, Kuo SH (1992) Value of sonography in determining the nature of pleural effusion: analysis of 320 cases. Am J Roentgenol 159:29–33

Yokoi K, Moro K, Miyazawa N, Saito Y, Okuyama A, Sasgawa M (1991) Tumor invasion of the chest wall and mediastinum in lung cancer: evaluation with pneumothorax CT. Radiology 181:147–152

Zerhouni EA, Scott WW, Baker RR, Wharam MD, Siegelman SS (1982) Invasive thymomas: diagnosis and evaluation by computerized tomography. J Comput Assist Tomogr 6:92–100

Ziter FMH Jr, Wescott JL (1981) Supine subpulmonary pneumothorax. Am J Roentgenol 137:699